Optimisation and Performance Evaluation in image registration technique

Shadrack Mambo

OPTIMISATION AND PERFORMANCE EVALUATION IN IMAGE REGISTRATION TECHNIQUES

by

Shadrack Mambo

Submitted in partial fulfilment of the requirements for the degree

DOCTOR TECHNOLOGIAE: ELECTRICAL ENGINEERING

in the

Department of Electrical Engineering

FACULTY OF ENGINEERING AND THE BUILT ENVIRONMENT

TSHWANE UNIVERSITY OF TECHNOLOGY

Supervisor : Prof. Karim Djouani
Co-Supervisors : Prof. Yskandar Hamam
Prof. Barend Van Wyk
Prof. Patrick Siarry

February 2017

DECLARATION

"I hereby declare that the thesis submitted for the degree D'Tech: Electrical Engineering, at the Tshwane University of Technology, is my own original work and has not previously been submitted to any other institution of higher education. I further declare that all sources cited or quoted are indicated and acknowledged by means of a comprehensive list of references".

S.F.M. Mambo.

DEDICATION

This work is dedicated to my late father Mr. Ibrahim Mambo Ng'ang'a, my Mother Dorcas Wambui, my beloved wife Rose Njeri, my daughter Kristine Wambui, my grandson Henry Maina and to Almighty God.

ACKNOWLEDGEMENTS

My sincere gratitude goes to Professors Karim Djouani, Yksandar Hamam, Barend Van Wyk and Patrick Siarry for their invaluable time, encouragement, guidance, patience and dedication to my research, which has made this work realisable.

The author of this thesis gratefully appreciates the contribution of Tshwane University of Technology (TUT) and the French South African Institute of Technology (F'SATI) for providing all the relevant and necessary support for this research. I shall not forget the exemplary service of Ms Adri Coetzer at the Faculty of Engineering and the Built Environment.

I am extremely grateful to God for His graciousness and blessings, without which this work would not have been possible. I am very grateful to my mother Dorcas Wambui, my mother in-law Alice Mbugua and all our siblings for their constant encouragement and prayers. Very special thanks go to my wife Rose, for her unwavering support, encouragement and companionship on every step taken during this research and all her efforts to ensure a conducive and comfortable environment. Wambui and Maina made it their point to call every week to check on how we are fairing on through out the entire period of the research. That kept the zest and fire to succeed burning and has not been taken for granted. I am very thankful to you both.

ABSTRACT

Recent research in image registration techniques has demonstrated its worth in a variety of fields from remote sensing to medical imaging. Image registration methods consist of having two input images named as scene and model being made points. This is followed by a registration transformation that relates the two images and similarity metric function that aims to measure a qualitative value of closeness or degree of fitting between the transformed scene image and the model image. Finally, an optimiser which seeks the optimal transformation inside the defined solution search space is performed. The main contribution of this research is to consider the theoretical convergence condition of optimisation and use it to derive an image-driven selection mechanism for free parameters. The main objective of this research is to apply optimisation methods in image registration techniques in order to provide the user with an estimate as to how accurate the registration actually is. The specific objectives will be to determine the transformation model, the similarity metrics in image registration and carry out a careful validation of performance in registration using known basic error classes and methods for measuring registration accuracy and robustness.

TABLE OF CONTENTS

LIST OF FIGURES

LIST OF TABLES

GLOSSARY

ANN	Artificial Neural Network
BFGS	Broyden-Fletcher-Goldfarb-Shannon
CBCT	Cone Beam Computer Tomography
CC	Correlation Coefficient
CGD	Conjugate Gradient Descent
CMA	Covariance Matrix Adaptation
CS	Continuous Space
CT	Computed Tomography
CVS	Computer Vision Systems
DS	Discrete Space
EA	Evolutionary Algorithm
ECC	Entropy correlation coefficient
EMPIRE	Evaluation Methods for Pulmonary Image Registration
EO	Evolutionary Optimisation
ES	Evolutionary Strategies
FFD	Free Form Deformation
GIS	Geographic Information System
IP	Image Processing
JE	Joint Entropy
JPDF	Joint Histogram and Joint Probability Distribution
L-BFGS	Limited memory Broyden-Fletcher-Goldfarb-Shannon
LDDMM	Large Deformation Diffeomorphic Metric Mapping
MI	Mutual Information
MRF	Markov Random Field
MRI	Magnetic Resonance Imaging
MSE	Mean Square Error
NN	Neural Network
NMI	Normalised Mutual Information
PET	Positron Emission Tomography
PIU	Partition Intensity Uniformity
RANSAC	Random Sample Consensus
RGB	Red Green and Blue
RIU	Ratio-Image Uniformity
ROI	Region of Interest
RSGD	Regular Step Gradient Descent
SAD	Sum of Absolute Differences
SIFT	Scale Invariant Feature Transform
SOM	Self-Organising Maps
SSD	Sum of Squares Differences
TME	Too Many Elements
TPS	Thin-Plate Spline

CHAPTER 1. INTRODUCTION

1.1 Image Processing

Image processing is a highly researched field due to its many areas of application such as medical imaging, Geographical Information System (GIS) and mapping, satellite communications, biomedical engineering, robotics, remote sensing, among others. It encompasses image registration, image segmentation and edge detection, image enhancement and restoration, image compression and pattern recognition. The importance of medical imaging as a core component of several medical application and healthcare diagnosis cannot be over emphasised. Integration of useful data acquired from different images is vital for proper analysis of information contained in the images under observation. For the integration process to be successful, a procedure referred to as image registration is necessary.

1.2 Image Registration Model and Framework

The purpose of image registration is to align two images in order to find a geometric transformation that brings one image into the best possible spatial correspondence with another image by optimising a registration criterion. The two images are known as the moving image and the fixed image. Image registration methods consist of having the two images referenced with control points. This is followed by a registration transformation

that relates the two images and a similarity metric function that aims to measure the qualitative value of closeness or degree of fitness between the moving image and the fixed image. Finally, an optimiser which seeks an optimal transformation inside the defined solution search space is performed. The optimal transformation T: $(x, y, z) \mapsto (x^{'}, y^{'}, z^{'})$ maps any point in the moving image $I(x, y, z, t)$ at a time t into its corresponding point in the fixed image $I(x^{'}, y^{'}, z^{'}, t_0)$ taken at time t_0. Since the motion of lung is non-rigid, correction of global and local deformations requires a combined transformation that consists of a global transformation and a local transformation, which is expressed as follows:

$$\mathbf{T}_(x, y, z) = T_{global}(x, y, z) + T_{local}(x, y, z) \tag{1.1}$$

Image registration consists of three major components namely,

1. The transformation model,

2. The similarity metric that describes the objective function to be minimised, and

3. The optimisation algorithm, which is the numerical method used to solve the minimisation problem.

The transformation models are classified into three categories according to:

1. Physical model,

2. Interpolation theory, and

3. Based on a prior knowledge.

Similarity metric component can be classified into three categories:

1. Geometric methods ,

2. Iconic methods, and

3. Hybrid methods, which combines the first two methods.

Optimisation algorithm as the last component can be categorised into:

1. Continuous methods such as gradient descent, conjugate gradient descent, Quasi-Newton and stochastic gradient;

2. Discrete methods which are methods based on graph theory and linear programming methods, and

3. Evolutionary and greedy algorithms.

The parameters that describe a geometric transformation can be computed directly or searched for. Extensive research done in image registration methods can be found in the following literature: Klein et al. (2010), Markelj et al. (2012) and Wang et al. (2001). The framework for image registration takes the form of Fig.1.1. Intensity-based image registration can be viewed as a non-linear optimisation problem which is expressed as:

$$\hat{\mu} = \arg\max_{\mu} C(I_f(\mu), I_m(\mu);\ T) \tag{1.2}$$

where C is the cost function or the similarity metric that measures the similarity between the fixed image I_f and the deformed moving image I_m. The solution is the parameter vector that minimises the cost function and T is the transformation. Non-parametric image registration methods use deformation fields to define the transformation relating to two images. In order to ensure that a smoothing function is available and that the non-parametric registration problem is well posed, a regularisation term must be added to the similarity measure to form the cost function. The process of minimising

the cost function is an optimisation problem which can be modelled mathematically. In its simplest form, an optimisation problem consists of minimising a real function by systematically choosing input values from within an allowed data set and computing the value of the function. An optimisation problem can be represented in the following way:

Given: a function f: $A \longrightarrow R$ from some set A to the real numbers.
Sought: an element $x_0 \in A$: $f(x_0) \leq f(x)\ \forall\ x \in A$ gives a minimisation solution. Typically, A is some subset of the Euclidean space R^n, often specified by a set of constraints that the members of A have to satisfy. The domain A of f is called the search space, while the elements of A are called candidate solutions. The function f is called the cost function and a feasible solution that minimises the cost function is the optimal solution.

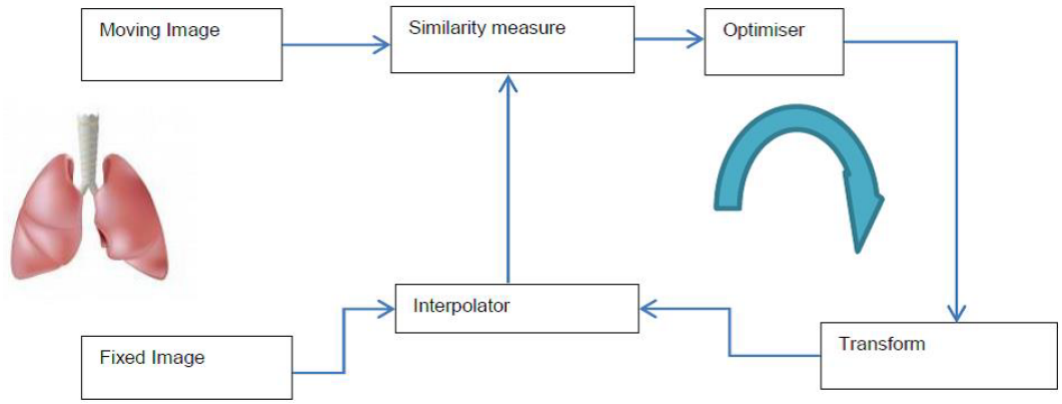

Figure 1.1: Image registration framework.

Fig.1.1 describes the image registration framework where the moving image is taken through a similarity measure such as mutual information to check quality of alignment. If the image is not aligned with reference to the fixed image, a fitness value is given. The image is then optimised, given new transform parameters and then passed through the interpolator until the degree of fitness to the fixed image is received. The semi-circle at the top right corner indicates that optimisation is a cyclic process. (NB: The image is a lung obtained from a data repository).

1.2.1 Transformation

1.2.1.1 Similarity Transformation

In the class of well-known transformation functions is similarity transformation, which is also known as the transformation of the Cartesian coordinate system. Similarity transformation relates coordinates of corresponding points in images when the moving image is translated, rotated and scaled with respect to the fixed image. It is defined by:

$$X = xs\cos\theta - ys\sin\theta + h \tag{1.3}$$

$$Y = xs\sin\theta + ys\cos\theta + k \tag{1.4}$$

where s is the scale, θ is the orientation or angle of rotation, and (h, k) is the location of coordinate system origin of the moving image with respect to the fixed image. This can be written in matrix form as:

$$\begin{bmatrix} X \\ Y \\ 1 \end{bmatrix} = \begin{bmatrix} 1 & 0 & h \\ 0 & 1 & k \\ 0 & 0 & 1 \end{bmatrix} \begin{bmatrix} cos\theta & -sin\theta & 0 \\ sin\theta & cos\theta & 0 \\ 0 & 0 & 1 \end{bmatrix} \begin{bmatrix} s & 0 & 0 \\ 0 & s & 0 \\ 0 & 0 & 1 \end{bmatrix} \begin{bmatrix} x \\ y \\ 1 \end{bmatrix}$$

or simply by

$$P = TRSp \tag{1.5}$$

where T is the translation, R is the rotation and S is the scale. Parameters s, θ, h and k are easily determined if a minimum of two corresponding points in the images are known.

1.2.1.2 Affine transformation

All linear operations such as translation, rotation, scaling and shearing are expressed through the same mathematical operation of matrix multiplication. Homogeneous coordinates are used to achieve this. The operation such as rotation about the origin through angle θ, scaling in 2D and shearing in x and y directions can be expressed using 2 x 2 matrix form shown below:

$$T_\theta = \begin{bmatrix} cos\theta & sin\theta \\ -sin\theta & cos\theta \end{bmatrix} \quad T_{sc} = \begin{bmatrix} s & 0 \\ 0 & s \end{bmatrix} \quad T_x = \begin{bmatrix} 1 & 0 \\ \alpha & 1 \end{bmatrix} \; and \quad T_y = \begin{bmatrix} 1 & \alpha \\ 0 & 1 \end{bmatrix}$$

where the scalars s and α are scaling and shear factors respectively. The operation of point translation is expressed through a single matrix multiplication with a vector addition as indicated below:

$$\begin{bmatrix} x' \\ y' \end{bmatrix} = \begin{bmatrix} x \\ y \end{bmatrix} + \begin{bmatrix} \alpha_x \\ \alpha_y \end{bmatrix}$$

or simply expressed as $x' = x + d$.

Point Distribution Matrix (PDM) S in a homogeneous system is defined by an augmented matrix as expressed below:

$$S = \begin{bmatrix} x_1 & x_2 & x_3 & ..... & x_N \\ y_1 & y_2 & y_3 & ..... & y_N \\ 1 & 1 & 1 & ..... & 1 \end{bmatrix}$$

In homogeneous coordinates, the affine transformation can be expressed as:

$$T = \begin{bmatrix} \alpha_{11} & \alpha_{12} & \alpha_{13} \\ \alpha_{21} & \alpha_{22} & \alpha_{23} \\ 0 & 0 & 1 \end{bmatrix}$$

where the parameters α_{13} and α_{23} correspond to the translation parameter.

From the aforementioned, the transformed shape coordinates $\hat{S}$ can be expressed as

$\hat{S} = TS$

where $T = T_1 T_2 \cdots T_N$ is a single matrix that operates on an input distribution S.

1.2.1.3 Projective transformation

Projective transformation is the transformation used in mapping of points on the object to corresponding points in the image into an arbitrarily oriented image plane. To completely determine the form of projective transformation, one considers how one arbitrary quadrilateral in the object maps into another quadrilateral in the image plane.

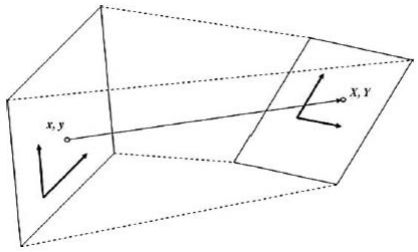

Figure 1.2: Projective Transformation.

Figure 1.2 shows projective transformation where (x, y) are the image plane coordinates and (X, Y) are referred to as the world coordinates of the object point.

The projective transformation has eight degrees of freedom because its mapping is constrained to four 2-D points. In the homogeneous coordinate system, the general form of projective transformation is given by:

$$T = \begin{bmatrix} \alpha_{11} & \alpha_{12} & \alpha_{13} \\ \alpha_{21} & \alpha_{22} & \alpha_{23} \\ \alpha_{31} & \alpha_{32} & \alpha_{33} \end{bmatrix}$$

Projected coordinates in the image plane are derived by matrix multiplication and relates to the world points. The transformed shape coordinates $\hat{S}$ is expressed as indicated below:

$\hat{S} = TS$ which gives:

$$\begin{bmatrix} x_1^{'} & ..... & x_N^{'} \\ y_1^{'} & ..... & y_N^{'} \\ 1 & 1 & 1 \end{bmatrix} = \begin{bmatrix} \alpha_{11} & \alpha_{12} & \alpha_{13} \\ \alpha_{21} & \alpha_{22} & \alpha_{23} \\ \alpha_{31} & \alpha_{32} & \alpha_{33} \end{bmatrix} \begin{bmatrix} x_1 & ..... & x_N \\ y_1 & ..... & y_N \\ 1 & 1 & 1 \end{bmatrix}$$

The reason there are eight and not nine degrees of freedom in projective matrix is that the parameters are constrained by the relation:

$$\alpha_{31}x + \alpha_{32}y + \alpha_{33} = 1 \tag{1.6}$$

1.2.2 Mutual Information

Mutual Information (MI) defines the amount of information that one image A contains about a second image B, based on the concept of information theory and expressed as follows:

$$C_{similarity}(A, B) = H(A) + H(B) - H(A, B) \tag{1.7}$$

where $H(A)$, $H(B)$ represent the marginal entropies of A, B and $H(A, B)$ represents joint entropy.

This research presented an automated image registration algorithm for solving multi-modal image registration on lung Computed Tomography (CT) scan pairs, where a comparison between regular step gradient descent optimisation technique and evolutionary optimisation was investigated. The aim of this research was to carry out optimisation and performance evaluation of image registration techniques in order to provide medical specialists with estimation on how accurate and robust the registration process was. Lung CT scan pairs were registered using mutual information as a similarity measure, affine transformation and linear interpolation. In order to minimise the cost function, an optimiser, which seeks the optimal transformation inside the defined search space was applied.

Determination of a transformation model that depends on transformation parameters and identification of similarity metric based on voxel intensity were carried out. By fitting transformation to control points, three transformation models were compared. Affine transformation produced the best recovered image when compared to non-reflective similarity and projective transformations. The results of this research compared well with documented results from EMPIRE 10 Challenge research and conformed to both theoretical principles as well as practical applications.

1.3 Optimisation-Based Registration

The aims of optimisation based registration are:

1. Definition of similarity or dissimilarity measure,

2. Identification of initial parameters that approximately register the images, and

3. Development of an algorithm that takes the initial registration to the final one.

An optimal registration is one that maximizes a similarity measure or minimises dissimilarity measure between images. The properties of the images under consideration for registration assist in choosing proper similarity or dissimilarity measure.

Specification of initial transformation parameters may be done interactively or determined automatically. In the interactive procedure, the user drags one image over the other to align them. The automatic method does not require user intervention. Images acquired in different modalities require that the entire parameter space be searched with relatively large steps in order to find best correspondence that can be used for initial registration. If the images are from the same modality, the initial registration will easily be achieved through alignment by applying the principal axes method. The optimal registration is achieved by iteratively refining the initial registration parameters until maximum similarity or minimum dissimilarity is reached.

Several optimisation approaches with convergence analysis have been proposed in the literature, as well as performance evaluation methods. The most commonly used optimisation algorithm are Powell-Brent, quasi-Newton, regularised step-size gradient descent, standard gradient descent, adaptive stochastic gradient descent, downhill simplex, simulated annealing and evolutionary strategies as presented by Gupta et al. (2012). However, not a single algorithm can be applied as standard method to all cases of image registration techniques. In their research, Van der Bom et al. (2011) have shown that the influence of optimisation methods on intensity-based 2D-3D image registration has not been investigated. They proposed that the registration criterion be formulated as a similarity measure defined in the multidimensional space of searched parameters. To bring the registration parameters within the capturing range of local optimisation methods, global optimisation approaches and heuristic search strategies are proposed. Accurate registration is a crucial pre-processing step for many tasks as suggested by Dura et al. (2012). Evaluation performance of registration techniques is therefore a necessary step

as proposed by de Groot et al. (2013), Dura et al. (2012) and Murphy et al. (2009). In their research, Floca & Dickhaus (2007) provide a framework offering suitable tools for an easy integration, optimisation and evaluation of registration approaches. The minimisation of the cost function in solving optimisation problems will be carried out.

1.4 Artificial Neural Networks

Artificial Neural Network (ANN) is a highly parallel system [Heger] composed of simple processing elements with complex global behaviour designed to produce intelligent solutions. ANN take input data values which are executed through a series of function to produce one or more output values Heger (2014). Among the many areas of application for ANN systems are pattern recognition, robotics, development of image processing algorithms and techniques, intelligence in business, to mention but a few.

There are several types of ANN in use for different purposes in image processing. These are classified according to area of application such as pre-processing, feature extraction, segmentation, classification, data compression and optimisation as indicated by Ramírez-Quintana et al. (2012). The common types of ANN used in image processing are:

1. Feed Forward Neural Network,
2. Self-Organising Maps (SOM),
3. Feed Forward Radial Basis Function Network (RBFNN) and
4. Hopfield Neural Network (HNN).

Feed forward neural networks are simple with neurons or connections from input layer connected to zero or hidden layers and finally to the output layer as discussed by Heger (2014). They are normally trained on genetic algorithms, simulated annealing or via any

propagation techniques. SOM is a neural network with two layers and its output layer employs a winner takes it all principle. The consideration is that the neuron with the highest output is the winner. HNN and RBF networks are used for pattern recognition. They are trained via algorithms that assist them to recognise patterns.

Neural network models used to find solutions for problems in image processing are very fast compared to conventional image processing methods. However, the time required to train a neural network is high, notwithstanding the complex computation of image processing tasks. An ANN requires a larger number of training data in order to achieve high and reliable results for performance of non-training subjects as suggested by Shi & He (2010). In this research, we created more data by performing translation, rotation and scaling on the lung CT scans dataset obtained from EMPIRE 10. These data were trained via ANN algorithms to assist in image registration. (NB: Further details will be provided once the results from simulation by Prof. Karim are available.).

1.5 Performance Evaluation of Registration Methods

The images under considerations have been acquired under different modalities. Joint Probability Density (JPD) of images contain information about the quality of registration for images from different modalities. The intensities of corresponding voxels in registered images form a JPD with a narrow band when the registration is accurate. JPD obtained for a registration that was not accurate will contain a wider distribution. Joint entropy (P) and joint energy (E) are measures used to quantify the spread of a probability distribution and are represented by the following expressions respectively:

$$P = -\sum_{i=0}^{255}\sum_{i=0}^{255} p_{ij}\log_2\left(p_{ij}\right) \tag{1.8}$$

$$E = \sum_{i=0}^{255} \sum_{i=0}^{255} p_{ij}^2 \tag{1.9}$$

These measures are used to quantify registration accuracy and the smaller the P (the larger the E) is, the better the registration will be for images in different modalities or in the same modalities respectively. Qualitative measure of registration accuracy can be done by an expert through visual evaluation alone. It is the method of choice for acceptance or rejection of results of an automatic registration procedure.

1.6 Importance/Benefits of Study

Image registration has a wide range of application especially in medical imaging. Available literature on image registration techniques indicate that there is no single method that is applicable to all cases of image registration. The study on different anatomical structure for image registration using non-rigid registration has not received a lot of attention in research. The aim of this research is to carry out optimisation and performance evaluation of image registration techniques. This will help identify parameters required, carry out optimisation and performance evaluation of the registration techniques employed. The data obtained from analyses of this research will provide physicians and clinicians with estimation as to how accurate the registration process actually is, as well as indicate the most accurate and robust registration techniques.

1.7 Delimitation of Study

This thesis will involve searching through current literature to investigate the status of existing methods for non-rigid medical image registration. Tools used will be laptop Intel Core i7 pre-loaded with necessary software such as Matlab and Latex among others.

The particular area of study will be image registration of lung CT scan using regular step gradient descent optimisation algorithm for medical imaging obtained from data repository by EMPIRE 10 challenge. This study does not intend to cover other anatomical human or animal body organs such as heart, brain, kidneys or liver but the method can be modified to suit them. Results of this study will assist medical doctors, physicians and clinicians quickly and accurately diagnose changes in internal body organs thereby delivering the fastest decision to save lives.

1.8 Contribution

The contribution of this research was its potential to increase the scientific understanding of image registration of anatomical body organs. It laid a basis for further research in performance evaluation of registration techniques. Validation of these procedures to other types of algorithms and image registration application areas, such as remote sensing, satellite communication, biomedical engineering, robotics, geographical information systems and mapping, among others are recommended for future research. The use of evolutionary optimisation algorithms combined with gradient descent optimisations improve speed and accuracy of registration when registering CT scans from lung images.

1.9 Organisation of Thesis

Research presented in this thesis is divided into 5 chapters. Chapter 1 covers introduction while chapter 2 discusses literature review of different image registration techniques, transformation models, similarity measures, interpolation and optimisation techniques. In chapter 3, a chronology of the methodology is given which details the use of mean squared differences and mutual information as similarity metrics and the optimisation techniques employed in lung CT scans registration. Chapter 4 focuses on analysis and

discussion of results. The thesis is concluded in chapter 5 with a conclusion and recommendations of future research.

CHAPTER 2. LITERATURE REVIEW

2.1 Introduction

This thesis has a foundation from scientific work in the fields of Medical Imaging and Computer Vision. Research presented in this thesis has wide areas of application not limited to medical imaging only. Image registration is commonly formulated as an optimisation problem based on an objective function which evaluates the quality of transformation with respect to the image data and some prior information. Registration is a problem that seeks to align two images in the same space or coordinates to achieve the best correpondences between them. There are several image registration techniques, whose use depend on area of application, image modality, time of image acquisition among other factors. Some of these techniques like intensity-based, control point-based, feature-based, elastic-based and neural network-based registrations have been discussed in this chapter. Literature review on different research topics related to image registration such as transformation models, similarity measures, interpolation and optimisation techniques have been presented in the literature review section. Literature review aims to provide a solid theoretical foundation for research endeavours in image registration techniques. Developing a solid foundation for a research study is possible through a methodological analysis and synthesis of existing contributions as discussed by Levy & Ellis (2006). A methodological analysis is crucial in understanding the existing body of knowledge including where excess research exists and where new research is needed. Out

of these considerations, the aim of this chapter is to enhance the scientific community's understanding of the current status of research in optimisation and performance evaluation of image registration techniques and also communicate to them, the contribution of this research in the field of image processing.

This chapter is divided into seven sections. The first section covers the introduction. The second section addresses literature review on image registration techniques. Section three looks at review on transformation models. The fourth section covers the overview on similarity measures. The fifth section contains literature review on various interpolation methods. Section six covers review on five types of optimisation techniques while the seventh section deals with performance evaluation.

2.2 Overview of Image Registration Techniques

By definition, image registration is the process of aligning a target image to a source image in order to determine the transformation that best maps points on the target image to corresponding points on the source image.

The purpose of carrying out image registration is to determine analysis of temporal evolution, fusion of multi-modal images, inter-patients comparison, atlas superposition and reconstruction of a 3D volume from a series of contiguous 2D slices from an Electron Microscopy camera. There are different classes of problems under image registration such as mono-modalities and multi-modalities images, intra-subjects or inter-subjects registration and rigid or non-rigid transformation. The process of image registration uses four steps namely: feature detection, feature extraction, transformation model estimation and registration of transformation model.

Image formation is the process where radiation emitted from an object is collected to form an image of the object in one or the other way. It includes geometric and radio-

metric aspects. The geometry of imaging requires the use of several coordinate systems such as world coordinates attached to the observed scene, the camera coordinates aligned to the optical axis of the optical system, the image coordinate related to the position on the image plane and the pixel coordinates attached to an array of sensor elements. In information theory, image synthesis consists of image registration and visualisation. Registration covers necessary processes that bring images into spatial alignment with each other. Visualisation on the other hand allows information from the aligned data sets to be observed together, for instance in montage. There are various reasons for performing image synthesis, among them being:

1. For assessment of diseases progression or growth using temporal series of images;
2. For combining of both structural and functional information acquired from different imaging modalities;
3. For comparing corresponding regions in different images or individuals by matching them into a standard coordinate system;
4. For generating and analysing atlases and or templates representing distinctive appearance in health or disease;
5. For providing a guideline to invasive procedures and image-guided surgery.

The position of objects in 3D space can be described in many different ways. We can use a coordinate system which is related to the observation scene. Coordinate mapping of corresponding points from world to camera coordinates, requires a translation and a rotation. First, the origin of the world coordinate system is shifted to the origin of the camera coordinate system by the translation vector T. Then the orientation of the shifted coordinate system is changed by a sequence of rotations about suitable axes so

that it coincides with the camera coordinate system. Mathematically, translation is described by vector subtraction and rotation by multiplication of the coordinate vector with a matrix:

$$X = R(X^{'} - T) \tag{2.1}$$

where X is the camera coordinate, $X^{'}$ is the world coordinate, T is the translation vector and R is the matrix.

Several methods have been proposed for medical image registration. According to Fitzpatrick et al. (2000), they are categorised into the following criteria: image dimensionality, nature of registration basis, geometric transformation, degree of interaction, optimisation procedure, modality, subject and object.

In this research, we are concerned with nature of registration basis, which is further subdivided into three major sections namely: intensity-based registration, control point-based registration and feature-based registration.

2.2.1 Intensity-based registration

In intensity-based registration, the voxel values alone are used to calculate transformation between two images. By iteratively optimising the cost function calculated using the pixel or voxel values, the registration transformation is determined. In medical imaging, 3D images are frequently used and therefore the cost function is referred to as voxel similarity measure or function. In many practical applications, intensity-based registration methods use only a subset of voxels and require some pre-processing procedures to be done. This may result in the algorithm running faster. The subset used may be chosen randomly or searched for, from a regular grid. In some cases of intensity-based registration methods, the cost functions work on derived image's parameters like image gradients

instead of the voxel values as shown by Fitzpatrick et al. (2000). Intensity-based registration methods have wide areas of application ranging from registering images with the same or different dimensionalities, intra-modality or inter-modality images to rigid transformation or deformable images. The similarity measures or cost functions used with intensity-based registration methods include: Sum of Squares Differences (SSD); Correlation Coefficient (CC); Ratio-Image Uniformity (RIU); Partition Intensity Uniformity (PIU); Joint Histogram and Joint Probability Distribution (JPDF); Joint Entrophy (JE); Mutual Information (MI) and Normalised Mutual Information (NMI).

2.2.2 Control Point-based registration

Control point-based registration provides for manual selection of common features in an image to map to the same pixel location. This method is best suited for images with distinct features. Correspondence establishment between detected set of candidate points in the target image and reference image is done using a searching procedure that minimises dissimilarity metric, as discussed by Wang et al. (2009). Control point selection *cpselect* is a four step process which starts as follows:

Step 1: Start the *cpselect* tool that specifies the target and reference images in Matlab.

Step 2: Use the navigation aid to scroll the image for landmark features common in both images. Functions such as panning, zooming, magnification and viewing other parts of the image can be carried out.

Step 3: Specify control point pairs that match the target image to the reference images.

Step 4: Save the control points to Matlab workspace.

2.2.3 Feature-based registration

Feature-based image registration detects feature points in both the fixed and moving images. It finds corresponding pairs and computes image transformation. Detectors such as Harris corner detector, Scale Invariant Feature Transform (SIFT) detector and Random Sample Consensus (RANSAC) are used in this registration. Feature-based image registration methods are used when local structure image data is much higher than data carried by image intensity, can handle complex distortions between images and are faster. They rely on relatively small number of features and do not evaluate a matching criteria for every single pixel. The general process includes identifying features in two images which are then paired to determine which feature in one image should be aligned to the other image. A calculation step then follows where the mathematical operation necessary to align sets of paired images is done. Finally application of transformation is done where the results of the calculations are applied to all pixels or voxels in one image that will be aligned with another image.

Registration algorithm has three main components namely the similarity measure, the transformation model (objective function) and the optimisation process. Result of the registration algorithm naturally depends on the similarity measure and the objective function. The dependency of the registration result on the optimisation strategy follows from the fact that image registration is inherently ill-posed as proposed by Sotiras et al. (2013). Enormous amount of research has been dedicated in the field of image registration which has generated many innovative ideas regarding the three algorithmic registration steps. Comprehensive scientific reviews in this field have been proposed in Sotiras et al. (2013), Markelj et al. (2012), Fluck et al. (2011), Ezzeldeen et al. (2010), Wyawahare et al. (2009) and Zitova & Flusser (2003). Image registration techniques are categorised based on geometric approaches, intensity-based approaches or the combination of both known as hybrid approaches, which has been presented by Gupta et al.

(2012). Geometric approaches have explicit models and fast optimisation procedures, are used for rigid or affine transformations and require user intervention to identify landmarks. The accuracy of registration is dependent on feature extraction steps. Intensity-based approaches match intensity patterns using a mathematical or statistical criteria, define measure of intensity similarity between source and target, and determines the transformation that optimises the voxel similarity measure. Hybrid approaches are a combination of both the geometric and the intensity-based approaches. They combine advantages of both geometric and intensity approaches to achieve more accurate registration.

Deformable models as discussed by Castillo et al. (2013) and Sotiras et al. (2013) can be used to take advantage of their strength, defined by large number of degrees of freedom, as well as allowing modelling of both misalignment between images and local deformations. Image registration techniques using deformable transformation models are very accurate and rectify local misalignment. Mathematical basis functions based on Fourier or Wavelet domain, are used in deformable transformation model to define the correspondence between the original image and the transformed image.

Multi-resolution methods offer powerful tools for signal analysis widely applied in feature extraction, image compression techniques and anti-noise applications as proposed by Vujović (2015). The main reasons why multi-resolution approach is used is to improve performance, reduce computational complexity, improve robustness, improve intuition and simplify the algorithm. Multi-resolution approaches and algorithms can be classified under the following three categories namely wavelet methods, Hierarchical models and Hierarchical algorithms. They are good for processes like feature extraction and filtering where Gaussian and Laplace filters are used.

2D-3D image registration methods do not require user interaction such as manual annotations, additional machinery or additional acquisition data as discussed by Van der Bom

et al. (2011). The same author recommended Powell-Brent search strategy for intensity-based 2D-3D image registration in cerebral interventions due to its good performance with all three similarity measures (gradient difference, gradient correlation and pattern intensity), and concludes his work by showing that further research on the influence of optimisation method on intensity-based 2D-3D image registration needs to be done.

2.2.4 Elastic Model-Based registration

In their research, Hopp et al. (2013) presented automatic multimodal 2D/3D breast image registration using biomechanical models and intensity-based optimisation. Accelerated non-rigid intensity-based image registration using Importance Sampling (IS), presented by Bhagalia et al. (2009) uses a small random subset of image voxels to approximate the gradient and reduces computation time. A two-step elastic medical image registration approach based on image intensity has been proposed by Wang et al. (2001). This approach has several attractive features such as achieving high registration performance and it is an automatic algorithm using the raw intensity as feature space. Other research based on elastic image registration has been developed by Klein et al. (2010) in the form of Elastix, a toolbox for intensity-based medical image registration. Another linear elastic model-based image registration algorithm is proposed by Lu et al. (2012), where robustness of the registration accuracy is the key finding.

In the research presented by Bunting et al. (2010), an approach for automatic image-to-image registration has been outlined, where a topologically regular grid of tie points was imposed within the overlapping regions of the images. This algorithm produced results that showed the automatic operator far outperformed the manual operator. However, some limitations of the network data structure were identified when dealing with very large errors. Volume image registration by template matching, suggested by Ding et al. (2001) involves comparing a given template with windows of the same size in an image

and identifying the window that is most similar to the template. The characteristics of this algorithm are that it computes correlation of the template with windows of the same size in the neighbourhood (auto-correlation) and also uses the eigenvalues of the inertia matrix of the template. A survey of medical image registration on graphics hardware has been carried out by Fluck et al. (2011), where an analysis of different approaches to programming on Graphics Processing Units (GPU), programming models and interfaces are presented. Researcher Kosiński et al. (2012) presented robust image registration based on mutual information measure and showed that it is a highly effective method for registration of multi-modal medical images.

2.2.5 Neural Network-based registration

Research carried out by Jiang et al. (2010) recommended future use of neural networks in medical image registration during pre-processing and post-processing stages. Computational intelligence with neural networks cover applications in medical imaging such as medical image registration, medical image content analysis used in edge detection, segmentation, breast cancer screening, and computer-aided detection and diagnosis as presented by Doi (2007). Neural networks are designed to find varying solutions through competitive learning, Self-Organising Maps (SOM) and grouping method or clustering to provide and process input features and give the best possible alignment during registration between different images or data sets. In the research by Zhang & Li (2007) surface-based rigid registration using neural networks demonstrated that registration systems could achieve sub-voxel accuracy compared to traditional methods and are significantly faster. Overall combining SOM with other registration techniques could result in very powerful registration algorithms. The area of neural networks as applied to medical image registration is open for future research and development.

Recently discovered 4D imaging techniques such as 4D-computed tomography (CT),

4D-Cone Beam CT (CBCT), 4D-Magnetic Resonance Imaging (MRI), and 4D-Positron Emission Tomography (PET) are effective tools used in spatial and temporal definition of tumor target volume in human anatomy. 4D-4D image registration research presented by Schreibmann et al. (2008) seeks to establish a spatio-temporal correspondence between a set of input images, finds the transformation matrix T(x, t) that maps an arbitrary point $[x, t]$ from the fixed image to the corresponding point $[\hat{x}, \hat{t}]$ on the moving image or vice versa. During the iterative optimisation of the metric function, the following basic operations on the moving image set are involved: translation in the x, y and z directions and in the temporal axis; non-uniform scaling in the x, y and z directions and in the temporal axis, and rotation in 3D space. Automated 4D-4D image registration as shown by recent research findings by Schreibmann et al. can find the best possible spatio-temporal match between two 4D data sets and is useful in all the 4D applications mentioned above.

2.3 Transformation Models

Transformation in image registration is defined as the coordinate mapping from the fixed image domain to the moving image domain, which can be expressed as:

$\mathrm{T}\colon\ \Omega_F \subset R^d \longrightarrow \Omega_M \subset R^d.$

The type of transformation model selected for specified image registration mainly depends on application and the kind of images being considered. For geometric transformation such as scaling, translation, shearing or rotation, linear transformation is the most suitable to align the images. In medical image applications where rigid structures are in consideration, linear transformation is applied. If the anatomical organ is expected to undergo changes in their form during image acquisition, then transformations

that can recover the deformations are applied, as suggested by Glocker et al. (2011).

Precise image registration is a crucial pre-processing step for many tasks in image registration techniques, which is presented by Dura et al. (2012). The fundamental characteristic of any image registration techniques is the type of spatial transformations or mapping used to properly overlay two images as shown by Deshmukh & Bhosle (2011). Several of these transformations exist such as rigid, affine, global, projective and perspective. The following are the types of transforms and their mathematical formulations commonly used in image registration:

Translation:

$$T_\mu(x) = x + t \tag{2.2}$$

Rigid or Euler Transform:

$$T_\mu(x) = R(x - c) + t + c \tag{2.3}$$

Similarity:

$$T_\mu(x) = sR(x - c) + t + c \tag{2.4}$$

Affine:

$$T_\mu(x) = A(x - c) + t + c \tag{2.5}$$

B-Spline:

$$T_\mu(x) = x + \sum_{x_k \in N_x} \rho_k \beta^3 \frac{x - x_k}{\sigma} \tag{2.6}$$

where,

$T_\mu(x)$ - is the transform;

t - is translation;

c - is a constant;

s - is similarity;

R- is rotational matrix;

A is matrix without restrictions;

x_k are control points;

p_k is B-Spline coefficient vector (control points displacement);

σ is B-Spline control point spacing;

N_x is set of all control points with the compact support of the B-Spline at x ;

$\beta^3(x)$ is the cubic multidimensional B-Spline polynomial.

Transformation model can be subdivided into rigid and non-rigid. Rigid registration finds the various degrees of freedom, namely three rotational and three translational forms of transformation that map any point in the source image into the corresponding points in the reference image. They are best used in applications where there is virtually little or no change in shape or location of the structure. Transformation parameters in 2D rigid transformation are discussed by Delibasis et al. (2011) in detail. Researchers Meskine et al. (2013) have developed a rigid point-set registration method based on the application of genetic algorithms and Hausdorff distance. The proposed method, unlike other methods that match two intensity images, can match a set of data extracted from an image. Non-rigid registrations are usually applied on imaged body organs which undergo soft-tissue type of deformation. Klein et al. (2006) made a comparison of accelerated techniques in medical image registration and introduced a fast non-rigid registration that allows online updating of treatment plan. Research using thin-plate spline non-rigid registration on images has been done by Brooks & Arbel (2007) and Bolin & Huihui (2010).

Diffeomorphism is defined as one-to-one, differentiable, invertible and smoothing mapping. Large Deformation Diffeomorphic Metric Mapping (LDDMM) is a framework in which the optimal velocity fields are time-dependent and geodesic as presented by Risser et al. (2010) and Arguillère et al. (2015). It statistically compares images and shapes,

as well as creation of atlases. LDDMM is a non-linear registration techniques that defines diffeomorphic transformations between images in which anatomical structures and sub-structures are maintained as indicated by Ceritoglu et al. (2010). This algorithm enhances registration accuracy and, by minimising the function of velocity field vector in deformation flow, it resolves registration between two images in an Euler-Lagrange framework by applying gradient descent, as demonstrated by Risser et al. (2010). Pai et al. (2014) presented step-wise inverse consistent Euler's scheme for diffeomorphic image registration. The challenges of LDDMM include memory and time consumption as well as practical use limited to small deformations even though designed for large deformations. Log-Demons or spectral Log-Demons uses spectral correspondence to find similarity between fixed image and moving image, as shown by Lombaert et al. (2013). The general Log-Demon framework comprises an input which has fixed image, moving image and an initial velocity field, and an output consisting of a transformation from the fixed image to the moving image, as presented by Lombaert et al. (2013).

Non-rigid registration using intensity-based similarity metric has been studied by Klein et al. (2010) and Van der Bom et al. (2011). In their research on non-rigid medical image registration method based on improved linear elastic model, Lu et al. (2012) proves that not only high registration accuracy is achieved, but also enhances robustness and anti-noise properties of the registration algorithm. Research on non-rigid registration of images for medical applications by Rueckert & Aljabar (2010) gave two drawbacks for non-rigid registration as speed and non-existence of a general standard method for assessing and evaluating the success of the registration techniques. The development of non-rigid registration techniques is an open area for further research and most algorithms are under different stages of evaluation and validation.

2.3.1 Non-reflective Similarity

Non-reflective similarity transformation which has four degrees of freedom and needs only two pairs of points supports rotation, translation and isotropic scaling. It is expressed as follows:

$$\begin{bmatrix} H \end{bmatrix} = \begin{bmatrix} h_1 & -h_2 \\ h_2 & h_1 \\ h_3 & h_4 \end{bmatrix}$$

The projection of a point $[x, y]$ by H is given by:

$$\begin{bmatrix} \hat{x} & \hat{y} \end{bmatrix} = \begin{bmatrix} x & y & 1 \end{bmatrix} \begin{bmatrix} H \end{bmatrix}$$

2.3.2 Affine Transformation

Affine transformation is any transformation that can be given in terms of matrix multiplications followed by vector addition. The value of pixel located at point coordinate $[\hat{x}, \hat{y}]$ in the output image is determined by the value of the pixel at coordinates $[x, y]$ in the input image. This can be expressed as:

$$\hat{x} = xh_1 + yh_2 + h_3 \quad and \quad \hat{y} = xh_4 + yh_5 + h_6 \tag{2.7}$$

where $h_1, h_2, ..., h_6$ are transformation coefficients. For one transformation, the transformation coefficients are:

$$\begin{bmatrix} H \end{bmatrix} = \begin{bmatrix} h_1 & h_4 \\ h_2 & h_5 \\ h_3 & h_6 \end{bmatrix}$$

which is a 3x2 matrix, or:

$$\left[H\right] = \begin{bmatrix} h_1 & h_2 & h_3 & h_4 & h_5 & h_6 \end{bmatrix}$$

which is a 1x6 vector.

For more than one transformation, the transformation coefficients are Q-by-6 matrix expressed as:

$$\left[H\right] = \begin{bmatrix} h_{11} & h_{12} & ..... & h_{16} \\ h_{21} & h_{22} & ..... & h_{26} \\ .... & ... & .... & ..... \\ .... & ... & .... & ..... \\ h_{Q1} & h_{Q2} & .... & h_{Q6} \end{bmatrix}$$

where Q is the number of transformations.

2.3.3 Projective Transformation

In projective transformation, the relationship between the input and output points is defined by the following equations:

$$\hat{x} = \frac{xh_1 + yh_2 + h_3}{xh_7 + yh_8 + h_9} \quad and \quad \hat{y} = \frac{xh_4 + yh_5 + h_6}{xh_7 + yh_8 + h_9} \tag{2.8}$$

where $h_1, h_2, ..., h_6$ are transformation coefficients. For one transformation, the transformation coefficients are arranged as a 3-by-3 matrix expressed as:

$$\left[H\right] = \begin{bmatrix} h_1 & h_4 & h_7 \\ h_2 & h_5 & h_8 \\ h_3 & h_6 & h_9 \end{bmatrix}$$

or as a 1x9 vector of the form:

$$\begin{bmatrix} H \end{bmatrix} = \begin{bmatrix} h_1 & h_2 & h_3 & h_4 & h_5 & h_6 & h_7 & h_8 & h_9 \end{bmatrix}$$

For more than one transformation, the transformation coefficients are arranged as Qx9 matrix expressed as follows:

$$\begin{bmatrix} H \end{bmatrix} = \begin{bmatrix} h_{11} & h_{12} & ..... & h_{19} \\ h_{21} & h_{22} & ..... & h_{29} \\ .... & ... & .... & ..... \\ .... & ... & .... & ..... \\ h_{Q1} & h_{Q2} & .... & h_{Q9} \end{bmatrix}$$

2.3.4 Thin Plate Spline Transformation

Thin plate spline, as shown by Goshtasby (2012), also referred to as surface spline is commonly used in non-rigid medical image registration as a transformation function, which is presented by Qiu et al. (2009) and Menon & Narayanankutty (2010) in their research. Together with Gaussian and multi-quadric functions, thin-plate spline form radial basis functions. Their common properties include providing optimally smooth deformations, are generally stable for weight estimation for different configurations of points, and are expensive to re-evaluate whole image match because a change of location on any landmark changes the whole deformation field. The thin-plate spline interpolating a set of points with associated values in a plane is defined by:

$$f(x, y) = A_1 + A_2 x + A_3 y + \sum_{i=1}^{n} B_i r_i^2 \ln r_i^2 \tag{2.9}$$

where, $r_i^2 = (x - x_i)^2 + (y - y_i)^2 + d^2$. The component d acts as a stiffness parameter, which, when increased, produces a smoother surface. Thin-plate spline is expressed in

terms of affine transformation and a weighted sum of radially formulated logarithmic basis functions, presented by Goshtasby (2012) as of the form $r_i^2 log r_i$.

2.4 Similarity Measures

Similarity measure is the second part of a registration process that computes the degree of alignment of the images. It can be categorised into two approaches, namely featured-based and voxel-based similarity measures. Feature-based approach, shown by researchers Han (2010) requires a feature extraction step which can bring an error that can generally affect the registration algorithm and cannot be reversed later, as indicated by Rueckert & Aljabar (2010). Voxel-based approach aims at determining the degree of similarity in the image intensities. Voxel similarity measures are generally preferred methods for measuring image similarity because of being robust and accurate. According to Van der Bom et al. (2011), the three similarity measures that give good accuracy and robust results are gradient descent, gradient correlation and pattern intensity. In their research, Klein et al. (2007) concluded that the choice of the characteristic of the cost function and the search strategy used determines how successful the registration process will become. Single modality image registration is best done using invariant moments while multi-modality image registration is best done using mutual information similarity measure. For images with rotational differences, cross correlation coefficients and invariant moments types of similarity measures are the best to apply. Mutual information similarity measure has highest sensitivity to image similarity, as presented by Yaegashi et al. (2013) because it is not calculated based on pixel by pixel value but by use of histogram of the gray scale values of two images.

2.4.1 Difference Measures

These type of similarity measures are the simplest and belong to a class of similarity measures known as point-wise measures as indicated in research done by Glocker et al. (2011). They are based on differences of intensities between the source and target images. The following two types will be considered:

1. Normalised Sum of Absolute Differences (SAD) is represented as:

$$S_{SAD}(I, J) = \frac{1}{|\Omega|} \sum_{p \in \Omega} |I(p) - J(p)| \tag{2.10}$$

and

2. Normalised Sum of Squared Differences (SSD) is represented as:

$$S_{SSD}(I, J) = \frac{1}{|\Omega|} \sum_{p \in \Omega} [I(p) - J(p)]^2 \tag{2.11}$$

where,

I is the source image;

J is the target image and

Ω is the image domain.

Intensity differences are applied in mono-modal registration where image acquisition is from same modality. They are easy to implement and compute efficiently. The difference between the two measures is that SAD is more robust to outliers while SSD over-penalises the outliers. Normalisation is done to ensure the measures are independent of the size of overlap of the domain Ω.

2.4.2 Statistical Measures

The most popular statistical measures include Correlation Coefficient (CC), Mutual Information (MI) and Entropy Correlation Coefficient (ECC) shown in the research by Glocker et al. (2011). CC is defined by the following expression:

$$S_{CC}(I,J) = \frac{\sum_{p\in\Omega}(I(p)-\mu_I)(J(p)-\mu_J)}{\sqrt{\sum_{p\in\Omega}(I(p)-\mu_I)^2}\sqrt{\sum_{p\in\Omega}(J(p)-\mu_J)^2}} = \frac{cov(I,J)}{\sigma_I\sigma_J} \tag{2.12}$$

where μ_I and μ_J are the two means and σ_I and σ_J are the standard deviations of the image intensity distributions. The correlation coefficient normally has values in the range [-1,1] where 1 indicates a perfect linear relationship, 0 indicates no relationship and -1 indicates inverse relationship. The CC criterion is driven by less strict assumptions on intensity relationship than difference measures. Mutual information is the statistical measure which goes beyond these assumptions and is given by:

$$S_{MI}(I,J) = H(I) + H(J) - H(I,J) \tag{2.13}$$

where $H(I)$ and $H(J)$ are marginal entropies and $H(I,J)$ is the joint entropy of the images I and J. The entropies are defined by the following expressions:

$$H(I) = -\sum_i p(i)\log p(i) \quad and \quad H(I,J) = -\sum_{i,j} p(i,j)\log(p(i,j)) \tag{2.14}$$

where $p(i)$ and $p(i,j)$ are the marginal and joint intensity distributions respectively. MI as a similarity measure requires more computational steps than the difference measures.

A popular and normalised version of mutual information is the entropy correlation coefficient which is expressed as follows:

$$S_{ECC}(I,J) = 2 - \frac{2H(I,J)}{H(I)+H(J)} \tag{2.15}$$

These types of statistical measures are used for multi-modal registration of CT and MRI images where no linear or even non-linear relationship between intensity distributions of images exist.

Below is a list of mathematical formulation for three similarity measures as shown by Kosiński et al. (2012): sum of absolute differences, cross correlation coefficient and mutual information.

a. Sum of absolute differences. Let f_1 represent a reference image, and f_2 represent a moving image. A similarity image, denoted by s with a location (x,y,z) can be expressed as (6):

$$s(x,y,z) = \sum_{i=1}^{n}\sum_{j=1}^{n}\sum_{k=1}^{n} \mathsf{f\_1(i,j,k)\text{-}f\_2(x+i\text{-}1,y+j\text{-}1,z+k\text{-}1)} \tag{2.16}$$

where,

x,y,z = 1,2,...,m-n+1.

b. Cross correlation coefficient can be expressed as (7):

$$s(x,y,z) = \frac{\sum_{i=1}^{n}\sum_{j=1}^{n}\sum_{k=1}^{n} f_1(i,j,k) - f_2(x+i-1,y+j-1,z+k-1)}{\sum_{i=1}^{n}\sum_{j=1}^{n}\sum_{k=1}^{n} f_1^2(i,j,k)^{1/2} \sum_{i=1}^{n}\sum_{j=1}^{n}\sum_{k=1}^{n} f_2^2(x+i-1,y+j-1,z+k-1)^{1/2}}. \tag{2.17}$$

where,

x,y,z = 1,2,...,m-n+1.

c. Mutual information can be expressed as (8):

$$I(T,W) = \sum_{a}\sum_{b} P_{TW}(a,b) log \frac{P_{TW}(a,b)}{P_T(a)P_W(b)} \tag{2.18}$$

where,

T is a template and W is a window and are both random variables;

$P_T(a)$ is the probability that the intensity at a voxel in T is a and

$P_W(b)$ is the probability that the intensity at a voxel in W is b;

$P_{TW}(a,b)$ is the joint probability, which gives the probability that intensity a in the template lies on top of intensity b in the window.

2.5 Linear Interpolation

Linear methods for interpolation can be divided into several groups such as neural networks, bilinear, bicubic, splines and sinc splines. Neural networks are the most basic, least time consuming during processing and deal with one pixel which results in making the pixels bigger. On the other hand, bilinear interpolation is a 2x2 neighbourhood that deals with 4 pixels and returns smoother images. Bicubic interpolation is a 4x4 neighbourhood that deals with 16 pixels, has sharper images and a combination of good computational time and quality. The splines and the sinc interpolations retain image information, are computationally extensive and useful for multiple image rotations and distortions. In interpolation, the formulation of problem statement is as follows: Given an input image k with uniformly-sampled pixels $p_{a,b}$, find a function $p(x,y)$ that satisfies:

$$p_{a,b} = p(a,b) \tag{2.19}$$

for all a, $b \epsilon Z$.

Sampling rate in interpolation must satisfy Nyquist Theorem. Interpolation computes values of a Continuous Space (CS) image $w_c(x,y)$ at (x,y) locations, matches them with values of a Discrete Space (DS) image $w_d(a,b)$, and gives corresponding samples of some continuous space image $w_c(x,y)$. Critical areas of application for interpolation include displaying, zooming, estimation of motion, coding and warping of images. These linear methods are expressed by the following mathematical formulation:

Linear interpolation:

$$w_c(x,y) = \sum_{n=-\infty}^{\infty} \sum_{m=-\infty}^{\infty} w_d[a,b] h(x - n\Delta_X, y - m\Delta_Y) \tag{2.20}$$

where $h(x,y)$ is the interpolation kernel.

2.5.1 Bilinear Interpolation

Bilinear interpolation is a tri function which is a piecewise linear function of its spatial arguments expressed as follows:

$$h(x,y) = tri(\frac{x}{\Delta_X}) tri(\frac{y}{\Delta_Y}) \tag{2.21}$$

In this scenario, for any coordinate point (x,y), the four nearest sample points are found as $w_d[0,0]$, $w_d[0,1]$, $w_d[1,0]$, $w_d[1,1]$. From there we fit a polynomial of the form:

$\alpha_0 + \alpha_1 x + \alpha_2 y + \alpha_3 xy$

The matrix representation of the above is given by:

$$\begin{bmatrix} 1 & 0 & 0 & 0 \\ 1 & 1 & 0 & 0 \\ 1 & 0 & 1 & 0 \\ 1 & 1 & 1 & 1 \end{bmatrix} \begin{bmatrix} \alpha_0 \\ \alpha_1 \\ \alpha_2 \\ \alpha_3 \end{bmatrix} = \begin{bmatrix} w_d[0,0] \\ w_d[0,1] \\ w_d[1,0] \\ w_d[1,1] \end{bmatrix}$$

2.5.2 Cubic Interpolation

Cubic interpolation is expressed by the following equation:

$$f(x) = \begin{cases} 1 - \frac{5}{2}|x|^2 + \frac{3}{2}|x|^3, & |x| \leq 1; \\ 2 - 4|x| + \frac{5}{2}|x|^2 - \frac{1}{2}|x|^3, & 1 < |x| < 2; \\ 0, & \text{otherwise.} \end{cases} \tag{2.22}$$

2.5.3 B-Splines Interpolation

Splines are piecewise polynomials with pieces that are smoothly connected together. For a spline of degree n, each segment is a polynomial of degree n. Splines are uniquely characterised in terms of a B-Spline expansion:

$$S(x) = \sum_{k \epsilon Z} c(k) \beta^n (x - k) \tag{2.23}$$

where $\beta^n(x)$ is the central B-spline

$c(k)$ represents B-Spline coefficients for discrete signals

B-Splines are symmetrical bell-shaped functions constructed from the $(n+1)$-fold convolution.

$$\beta^0(x) = \begin{cases} 1, & -\frac{1}{2} < x < \frac{1}{2}; \\ \frac{1}{2}, & |x| = \frac{1}{2}; \\ 0, & \text{otherwise.} \end{cases} \tag{2.24}$$

n-order B-Spline is expressed as follows:

$$\beta^n(x) = \frac{1}{n!} \sum_{k=0}^{n+1} \binom{n+1}{k} (-1)^k \left(x - k + \frac{n+1}{2} \right)_+^n \tag{2.25}$$

where

$$x_+^n = \begin{cases} x^n, & x \geq 0; \\ 0, & x < 0. \end{cases}$$

Cubic B-Spline basis function is a popular choice expressed in the form:

$$\beta^3(x) = \frac{1}{6}[(x+2)_+^3 - 4(x+1)_+^3 + 6(x)_+^3 - 4(x-1)_+^3 + (x-2)_+^3] \tag{2.26}$$

$$\beta^3(x) = \begin{cases} \frac{2}{3} - |x|^2 + \frac{|x|^3}{2}, & 0 \leq |x| < 1; \\ \frac{(2-|x|)^3}{6}, & 1 \leq |x| < 2; \\ 0, & 2 \leq |x|. \end{cases} \tag{2.27}$$

Interpolators have some desirable properties as listed below:

1. Self consistency:

$w_c(x,y)|_{x=n\Delta} = w_c(n\Delta) = w_d[n]$

2. Continuous and smooth:

$\frac{\partial}{\partial x} w_c(x,y) = \sum_{k=-\infty}^{\infty} w_d[n] \frac{\partial}{\partial x} h(x - n\Delta)$

3. Short spatial extent to minimise computation:

$w_c(x,y) = \sum_{k=-\infty}^{\infty} w_d[n] h(x - n\Delta) =$

$= \sum_{n \epsilon Z : x - n\Delta \epsilon S} w_d[n] h(x - n\Delta)$

4. Frequency response approximation.
5. Symmetric.
6. Shift invariant, and
7. Minimum side-lobes to avoid ringing artifacts.

2.6 Optimisation Techniques

The optimisation process is another component of image registration algorithm. Optimisation method is a procedure that finds various parameters that optimise a given similarity measure. A dependable optimiser will reliably and quickly find the best possible transformation. Registration via optimisation is a variational-based approach, as presented by Fischer & Modersitzki (2008) which allows a sound mathematical treatment, characterisation, formulation as well as classification of some of the most used procedures. Optimisation-based registration according to Goshtasby (2012) is classified according to the area to which deformations belong, either rigid or non-rigid. Rigid, sometimes referred to as affine, registration process depends on some selected few param-

eters, while spline-based approaches usually have very high-dimensional transformation area. During image registration, issues such as ill-conditioning, instability of solutions and non-convexity of the cost functions occur which can be alleviated by introduction of a regularisation and additional penalty term in the optimisation problem, as described by Fischer & Modersitzki (2008). Optimisation-based registration requires that a similarity or dissimilarity measure is defined, initial parameters that nearly register the images are found and an algorithm is developed to run the initial registration to completion, as shown by Goshtasby (2012). Some properties of images determine how well the proper measure of similarity or dissimilarity between two images is done. For example, images acquired in different modalities require mutual information to determine the similarities, and joint entropy to determine the dissimilarities. Images acquired in the same modality need cross correlation coefficient to measure similarity, and sum of squared differences to measure dissimilarity between them. Transformation parameters are either specified manually or automatically. The initial registration used is searched for within the entire parameter space to find the best approximate registration. Parameters for the initial registration are iteratively refined until the optimal registration is achieved.

The most commonly used optimisation algorithms are gradient descent as shown by Markelj et al. (2012), Powell as indicated by Van der Bom et al. (2011), quasi-Newton, non-conjugate gradient descent as given by Klein et al. (2006), stochastic gradient descent as presented in Klein (2008), downhill simplex and Marquardt-Levenberg as shown by Markelj et al. (2012). Recent research has produced other approaches like local perturbation Dasgupta et al. (2013), global optimisation approaches such as stochastic global optimisation Zhigljavsky & Žilinskas (2007), convex optimisation Boyd & Vandenberghe (2009), stochastic approximation Chen (2003), exploration or selection, sequential Monte Carlo techniques and library-based optimisation. Optimisation problems can be classified as deterministic and non-deterministic. In deterministic optimisation problems,

neither randomness nor uncertainty is taken into account as indicated by Chen (2010), though they are very simple to solve. However, in non-deterministic optimisation problems, which reflect actual optimisation problems, noise or uncertainties occur in the form of randomness. Stochastic optimisation is very useful during design, analysis and operation of modern systems.

Optimisation algorithms such as quasi-Newton methods as seen in Hennig & Kiefel (2013) require only the gradient of the objective function to be computed at each iteration, they are much faster than steepest descent and more efficient than Newton methods. The most commonly used quasi-Newton method is the Broyden-Fletcher-Goldfarb-Shanno (BFGS) as shown by researchers Blomgren (2014) and Lewis & Overton (2013). Quasi-Newton methods function well in the stochastic approximation domain by using limited memory BFGS (L-BFGS). In their research, Byrd et al. (2014) employed the second-order information which reliably yielded stable and productive Hessian approximations. Discrete optimisation as compared to continuous optimisation offers a lot of advantages. It performs as a Markov Random Field (MRF) labelling, which is an energy function consisting of two terms, namely the data term and the regularisation term. The data term measures the similarity of voxel in one image and a displaced voxel in the second image. The regularisation term is a pair-wise function that enforces a globally smooth transformation by penalising derivatives of the displacements and has a weighting parameter that sets the influence of the regularisation Ferrante & Paragios (2013). The advantages of discrete optimisation include overcoming susceptibility of local minima, eliminating need for numerical derivatives of the objective function and offering high accuracy and good computational speed as compared to what is commonly observed in continuous optimisation.

Optimisation problems seek to determine a configuration or design that minimises the

cost function as shown by Chen (2010):

$$min_{\theta \in \Theta} J(\theta) \tag{2.28}$$

where,

θ is a p-dimensional vector of all decision variables, commonly represented by x in mathematical programming, and Θ is the feasible region.

If the cost function $J(theta)$ is linear in θ, and Θ can be expressed as a set of linear equations in θ, then we have a linear program. Similarly, if $J(theta)$ is convex in θ and Θ is a convex set, then we have a convex optimisation problem, as presented by Klein et al. (2010). In their research, Klein et al. (2006) similarly defined the optimisation problem that seeks to minimise the cost function as:

$$minimise_{x \in R^n} := g(x) + h(x) \tag{2.29}$$

where,

g is a convex, continuously differentiable function and h is a convex but not necessarily differentiable penalty function or regulariser. The same author showed that proximal Newton-type procedures inherit the desirable convergence behaviour for minimising smooth functions. The minimisation of the cost function follows line search methods as per:

$$x_{k+1} = x_k + t_k \Delta x_k \tag{2.30}$$

where,

t_k denotes a scalar gain factor that controls the step size in the search direction;

Δx_k is the search direction at iteration k and means that several iterations of an algo-

rithm are carried out.

The search direction and the gain factors are chosen such that the sequence x_k converges to a local minimum of the cost function. Approaches towards stochastic simulation optimisation, presented by Chen (2010), such as model-based approaches and meta-heuristics can improve image registration processes because with reference to simulation optimisation, the handles associated with the search have been eliminated. Therefore, allocation of simulation replications to different or alternative designs can be carried out efficiently. Meta-heuristics starts with an initial population of designs. This approach can be used for performance evaluation when the design area is being searched for. This is because generation of a good population of designs requires that iteration to iteration in the search process be carried out.

Several research works on optimisation on image registration can be found in Van der Bom et al. (2011), Klein et al. (2007), Klein (2008), Lee et al. (2014), Klein et al. (2009), Baudin et al. (2010), de Groot et al. (2013), Delibasis et al. (2010), Kabus et al. (2004) and Klein et al. (2011). In their research work, Floca & Dickhaus (2007) designed a powerful tool whose framework uses an engine that compares different registration approaches and hence makes the tool suitable for easy integration, optimisation and evaluation. This tool contributes immensely in establishment and optimisation of image registration techniques due to its ability to be automated. As a result, a lot of time is saved in clinical application procedures. The research work by Klein (2008) in its contribution explains that the choice of optimisation procedure adopted significantly impacts on the computation time, accuracy and robustness of the registration method used, which in turn influences the clinical procedures and the turnaround time for diagnosis and therapy treatment.

This research is based on theoretical work done by Plakhov & Cruz (2004), where the theoretical convergence conditions of the optimisation algorithms are taken into con-

sideration. In Klein et al. (2009), a stochastic adaptive descent optimisation method for image registration with adaptive step size prediction is presented, which provides a solution to Robbin-Monro schemes shortcoming of the need for a predetermined step size function. The main advantage of adaptive stochastic gradient descent optimiser stems from the fact that random sampling of the data in the computation of the derivatives is utilised, which translates into a meaningful reduction of computation time. A comprehensive review of 2D/3D registration based on optimisation procedure has been proposed by Markelj et al. (2012) for image-guided interventions. An improvement on the intensity-based image registration can be viewed as a non-linear optimisation problem which is expressed as:

$$\hat{\mu} = \arg\max_{\mu} C(I_f(\mu), I_m(\mu);\ T) \tag{2.31}$$

where,

C is the objective function or similarity measure that compares the alignment between the source image I_f and the reference image I_m. The solution μ is the parameter vector that minimises the objective function and T is the transformation.

2.6.1 CMA Evolutionary Strategy Optimisation

Evolutionary optimisations adapt to biological process of optimisation known as evolution. They are based on evolutionary operators such as crossover, mutation and selection as shown by Kramer (2014). From a set of candidate solutions, the crossover evolutionary methods combine the best characteristics of two or more solutions. In mutation, random changes are effected while ensuring articulate balancing of exploitation and exploration. Selection uses iteration process to choose the most promising candidate solutions by recombination and mutation. Covariance matrix adaptation (CMA) evolutionary strategy

presented by Kramer (2014) is a very powerful evolutionary optimisation algorithm. It is commonly used where no derivatives are given and no assumptions about the fitness function are known. Proven success of these algorithms have been demonstrated through theoretical results and a large area of application in past research. However, this success is attributed to proper parameter settings before and during search. Evolutionary algorithm model as indicated by Mwaura & Keedwell (2010) are based on stochastic algorithms and follow the listed down steps as a general methodology for solutions to population based EA problems:

Step 1: Create an initial population of solutions $P(0) = (P_1(0), ..., P_n(0))$;

Step 2: Compute the fitness $f(P_i(t))$, for each individual $P_i(t)$, of the current population $P(t)$. $P_i(t)$ refers to an individual i in $P(t)$ and t is the number of generations;

Step 3: Select parent organism by applying selection method and/or replication;

Step 4: Apply genetic operations on parent individuals to create offspring $P(t+1)$ that make up the next generation or replace individuals in the current population, and

Step 5: Go to step 2; if maximum fitness has been achieved or maximum generation attained exit algorithm else go to step 3.

Three operations are carried out in all evolutionary optimisation methods namely, evaluation, selection and alteration as shown by Machowski & Marwala (2007). The application of these operations to different branches of EO such as Simulated Annealing (SA), Genetic Algorithms (GA) and Particle Swamp Optimisation (PSO) vary from algorithm to algorithm. Most traditional optimisation techniques make use of the cost function value from its first derivative or second derivative. EO algorithms do not apply any other information but cost function values themselves and by so doing, eliminates the need to evaluate the gradients which can be computationally expensive. They sample the search space in detail more than non-evolutionary methods, thereby increasing the probability of finding the global optimum point or local minimum. The main advantage of using

evolutionary computation in image registration is to help avoid the common challenges of classical gradient-based optimisation techniques as demonstrated by Valsecchi et al. (2012).

2.6.2 Regular Step Gradient Descent Optimisation

In Regular Step Gradient Descent (RSGD) optimisation, the step size is computed by use of bipartition scheme as presented by Wu & Murphy (2010) and Paquin (2007) where the parameters of transformation in the direction of the gradient are advanced and the step size is governed by learning rate, given in Eikvil et al. (2005) research. The gradient of a function is an n-component vector given by:

$$\left[\Delta \mathrm{f}_{n*1}\right] = \begin{bmatrix} \frac{df}{dx_1} \\ \frac{df}{dx_2} \\ \vdots \\ \frac{df}{dx_n} \end{bmatrix}$$

The gradient direction is also known as the direction of steepest ascent, which has a local property and not global one. The function value increases fastest along the tangent of descent for one point but varies from point to point along the direction of steepest ascent. Gradient vectors, $\Delta(f)$, is evaluated at points along the gradient direction that represent the direction of steepest ascent. The negative of a gradient vector shows the direction of steepest descent. For the proof of this, we refer reader to Appendix A1. The possibility of derivation of theoretical bounds on distance to the solution at an iteration gives an indication of the rate of convergence of gradient descent algorithm as discussed by Klein (2008).

2.6.3 Conjugate Gradient Descent Optimisation

Gradient descent is commonly used for large scale optimisation problems due to its simplicity in implementation and cheapness in iteration as presented by Hauser (2012). It consists of taking small steps in the direction of the steepest descent. This optimiser advances the parameters of transformation in the direction of the gradient and the step size is governed by learning rate. The setback for gradient descent algorithms is that the step size depends on the value of the gradient, which has been shown by Eikvil et al. (2005). Steepest descent method uses the principle of the negative vector as the direction of minimisation, according to Rao & Rao (2009). It is based on the first order of Taylor approximation of the form $f(x+u)$ around x expressed as:

$$f(x+u) \approx \hat{f}(x+u) = f(x) + \nabla f(x)^T u \tag{2.32}$$

where $\nabla f(x)^T u$ is the directional derivative of f at x in the direction of u as indicated by Boyd & Vandenberghe (2009), that gives an approximate change in f for a small step in u. When the value of the directional derivative is negative, the step u is the descent direction. It is desirable to make the directional derivative as negative as possible by taking large values of u. The directional derivative $\nabla f(x)^T u$ is linear in u as long as it is the descent direction of the form $\nabla f(x)^T u < 0$. There is need to set limit for the size of u which is referred to as normalisation of the length of u.

Let $\| \cdot \|$ be any norm on $\mathbf{R}^n$. We define the steepest descent direction (with respect to the norm $\| \cdot \|$) as:

$$\Delta x_{nsd} = argmin\{\nabla f(x)^T u \mid \| u \| = 1\} \tag{2.33}$$

From the foregoing, a normalised steepest descent direction Δx_{nsd} is a step of unit norm that yields the largest decrease in the linear approximation of f. It can also be defined

geometrically as:

$$\Delta x_{nsd} = argmin\{\nabla f(x)^T u \mid \| u \| \leq 1\} \tag{2.34}$$

which gives the interpretation the direction of the unit ball $\| \cdot \|$ that extends farthest in the direction $-\nabla f(x)$.

The steepest descent method applies the steepest descent direction as search direction, as shown by Boyd & Vandenberghe (2009). Conjugate Gradient Descent (CGD) method is used to improve the convergence characteristics of steepest descent method. Any minimisation method that uses conjugate direction is said to be quadratically convergent and ensures that minimisation of a quadratic function is done in n steps or less. A general function that can be approximated fairly well by a quadratic near the optimal point, finds the optimal point in a determined number of iterations.

2.6.4 Quasi-Newton Optimisation

Quasi-Newton methods, according to Lewis & Overton (2013) are the most popular of the BFGS methods which are optimisation algorithms that require only the gradient of the cost function to be computed at each iteration. They are faster than the steepest descent, much more efficient than Newton algorithms and operate in the stochastic approximation regime by using L-BFGS. Quasi-Newton methods construct and employ Hessian approximation for arbitrary smooth cost function $f(x)$ using the values of second-order information evaluated at the current and previous points, as proved by Byrd et al. (2014). Further, Quasi-Newton methods minimise the problem of a convex (non-convex) stochastic function which is expressed as follows:

$$\min_{\omega \in R^n} F(\omega) = E[f(\omega;\ \xi)] \tag{2.35}$$

where

ω is a random variable consisting of input-output pair (x, z);

x is the input representation;and

z is the target output.

The collection of $\{(x_i, z_i)\}$, i=1,.....,N is referred to as the training data set. The cost function is defined by the empirical expectation:

$$F(\omega) = \frac{1}{N} \sum_{i=1}^{N} f(\omega_i, x_i, z_i) \tag{2.36}$$

2.6.5 Discrete Optimisation

In discrete optimisation format, the variables have discrete values which are labelled to each variable such that the cost function is minimised. Such a discrete optimisation performs as an MRF, as presented by Zikic et al. (2010). An MRF is a probabilistic model which is expressed by undirected graph containing a set of vertices that encodes random variables, whose values are derived from a discrete set. The aim is to estimate the optimal label assignment by minimising an energy function in the form:

$$E(f) = \sum_{p \in D} D(f_p) + \alpha \sum_{(p,q) \in N} R(f_p, f_q) \tag{2.37}$$

where,

$D(f_p)$ is the data term (unary cost) that measures the similarity of voxel in one image and a displaced voxel in the second image;

$R(f_p, f_q)$ is pair-wise regularisation term that enforces a globally smooth transformation by penalising deviations of the displacements;
α is the weighting parameter that sets the influence of the regularisation, as indicated by Heinrich et al. (2012) and Ferrante & Paragios (2013).

Discrete optimisation is able to locate an approximate global optimum of the registration cost function and can avoid false local optima. It does not require second-order information of similarity metric which increases flexibility. The advantages of discrete optimisation are that it overcomes susceptibility of local minimum caused by continuous optimisation, eliminates requirements for numerical derivative of the cost function and has good accuracy and computational speed compared to continuous optimisation. The main challenges include avoidance of an iterative solution, image interpolation and requires intensive sampling of the displacement space which results in high computational and memory needs.

2.7 Performance Evaluation

Performance evaluation is the last component of image registration algorithm that analyses and validates how well a particular technique performed. There are various performance evaluation methods but we shall highlight expert judgement method, NUMERICS algorithms and OSIRIX software.

Expert judgement methods are based on identification and correlation of similar and shared anatomical structures between images, as shown by Adler (2011). Landmarks or segmented regions of interest are used to perform validation. Structures known to be shared across individuals in a population have their landmarks and segmented regions of

interest defined. The accuracy of registration algorithms that apply methods based on landmarks and ROI are basically limited to the accuracy in which these features can be identified. The limitation of human judgement is its subjectivity and the results yielded are difficult to reproduce. Further to that, these evaluations are unable to detect any registration mismatches that may exist between landmarks or within ROIs. The other challenge is in distinguishing between registration errors and real morphological variability within a study population. The advantages of expert judgement are that they provide better visual perception, quicker user recognition and interaction.

NUMERICS is a web software platform for evaluation of performance of registration techniques. It provides accessible tools that allow access to dedicated numerical methods for comparison and registration of medical images as presented by Gerganov et al. (2012a). NUMERICS platform supports two classes of image registration algorithms, namely standard image registration and elastics Thin-Plate Splines (TPS) image registration. Standard category which are based on parameter optimisation techniques allow selection of specific geometric transformation functions, specific cost functions and chosen optimisation algorithms. The TPS image registration is based on the thin-plate spline interpolation approaches where elastic deformation of the initial image is performed. Interpolating feature points displacements are done in the coordinate plane using thin-plate splines. The platform has two pages from where the user uploads the two images to be registered and also specifies the type and the parameters of the algorithms that will be used. Page two contains the dashboard which displays results from submitted job and a list of all the intermediate steps performed. Detailed statistical information that includes mean, median, minimum and maximum intensity, standard deviation of the intensities, 3rd and 4th moment of the distribution of the intensities and a histogram of the intensity distribution are given as shown by Gerganov et al. (2012a).

The advantage of the NUMERICS platform as a tool for evaluation of performance of image registration algorithm is that it provides processing operations for analysing the results. It produces rendering contours that give areas of statistical significance difference between submitted images. By applying different colour schemes to the images, an improved visualisation quality is displayed.

CHAPTER 3. METHODOLOGY

3.1 Introduction

Image registration is the process of aligning a target image to a source image in order to determine the transformation that best maps points in the target image to corresponding points in the source image. This process adds value to images in the sense that it allows structural and functional images to be observed and analysed in the same coordinate system. The registration process has wide areas of application such as monitoring of diseases in clinical applications, constructing of mathematical models in the study of population and developing geographical maps among other applications. In this research we carried out image registration of lung CT scans from EMPIRE 10 Challenge by applying Mattes mutual information as a similarity metric, affine transformation, linear interpolation and regular step gradient descent optimisation using Image Processing toolbox in Matlab. Matlab, which is an acronym from MATrix LABoratory (MATLAB) is a computational, analysis and programming tool. It is a high performance language for technical computing that integrates programming, computation and visualisation in solving matrix and vector-based problems in a very short period of time compared to other languages such as C and Fortran. Matlab consists of a family of application-specific solutions known as toolboxes, which are detailed collections of Matlab functions referred to as M-files used to solve specific classes of problems. In this research, we applied Image Processing, Computer Vision Systems (CVS), Neural Network and Optimisation

Toolboxes. Part two of the image registration process uses neural networks.

3.2 Image Registration Techniques

Image registration considers two images. One is the target image, denoted as I_f and the other is the source image denoted as I_m. The aim is to find a transformation T that best aligns the two images:

T:$\Omega_F \subset R^d \longrightarrow \Omega_M \subset R^d$,

where Ω is the image domain and R^d is the Euclidean distance of dimension d equal to 2 or 3. The source or moving image I_m will be deformed by a transformation T to fit the target or fixed image I_f. The deformed image is symbolised as $I_m \circ T$. If the energy or cost function C created to evaluate how well the target image I_f fits the deformed image $I_m \circ T$, then an expression for the best transformation will be:

$$\hat{T} = arg\, min_T C(T) \tag{3.1}$$

where,

C is the cost function or similarity measure that compares the alignment between the source image I_m and the target image I_f. The solution $\hat{T}$ is the parameter vector that minimises the objective function and T is the transformation.

The steps for proposed algorithm for image registration:

Step 1: Take the 1st set of lung CT scan images 01;

(a) Fixed Image 01 (b) Moving Image 01 (c) Fixed Image 02 (d) Moving Image 02

Figure 3.1: Fixed and Moving Image Pairs 03 and 04.

(a) Fixed Image 03 (b) Moving Image 03 (c) Fixed Image 04 (d) Moving Image 04

Figure 3.2: Fixed and Moving Image Pairs 03 and 04.

Step 2: Load the fixed and moving images;

Step 3: Find image rotation and scale;

Step 4: Resize the images to make them same size;

Step 5: Select Control Points (CP) for both fixed and moving images and save them in workspace;

Step 6: Estimate transformation;

Step 7: Choose the optimiser and the metric functions;

Step 8: Show the final registered image.

Fig. 3.1-3.3 show images acquired from the EMPIRE 10 database used for this registration:

The original images have diverse dimensions and therefore there is need to resize them

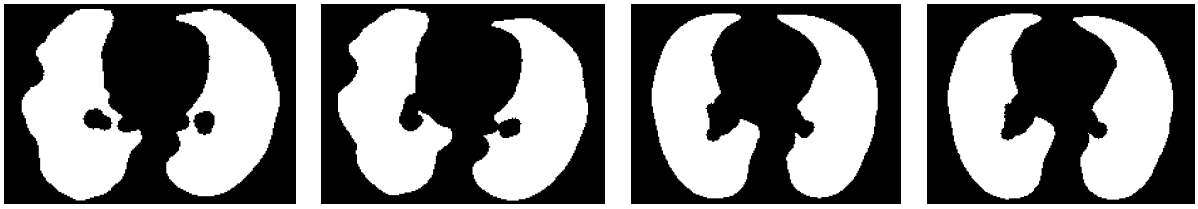

(a) Fixed Image 05 (b) Moving Image 05 (c) Fixed Image 06 (d) Moving Image 06

Figure 3.3: Fixed and Moving Image Pairs 05 and 06.

to 256 x 256 pixel sizes or less for them to be applicable in image processing toolbox applications. The next step is spatial transformation which brings the moving image into alignment with the fixed image. To apply a geometric transformation, parameters of transformation on the images are defined. This is done using affine transformation whose matrix's last column contains [0 0 1].

Registration can be divided into two forms, namely global and local registration. Global registration is based on block-matching techniques and finds similarities between sub-volumes of pairs of images for registration while local registration is based on Free Form Deformation (FFD) as proposed by Modat et al. (2010). Local registration consists of a deformation model, an objective function and the optimisation scheme.

Using the Image Processing (IP)and Computer Vision Systems (CVS) toolboxes in Matlab, three image registration solutions have been investigated, namely: intensity-based automatic registration, control point-based registration and automated featured-based registration. Depending on the relative intensity patterns, certain pixels are mapped to the same location in intensity-based automatic registration. In control point-based registration, manual selection of similar features in each image are allowed to be mapped to the same pixel location. Automated feature-based registration uses feature matching between images and involves feature detection, extraction and estimation of transformation. Transformation in image registration is defined as the coordinate mapping from the fixed image domain to the moving image domain. The mathematical model that

expresses transformation is given by:

$$X' = XR + T \tag{3.2}$$

The above can be represented in matrix form as:

$$\begin{bmatrix} x' \\ y' \end{bmatrix} = \begin{bmatrix} cos\theta & -sin\theta \\ sin\theta & cos\theta \end{bmatrix} \begin{bmatrix} x \\ y \end{bmatrix} + \begin{bmatrix} t_x \\ t_y \end{bmatrix}$$

The estimated rotational angle is a matrix containing equal values that can be found as per parametric representation of a line:

$$\rho = ycos\psi - xsin\psi \tag{3.3}$$

$$\rho' = y'cos\psi' - x'sin\psi' \tag{3.4}$$

Substituting (3.2) and (3.3) in the matrix above and using trigonometric theorem, we find that:

$$\theta = \psi' - \psi \tag{3.5}$$

Details of the procedure followed in registration of all images mentioned above are given in Appendix C.

Precise image registration is a crucial pre-processing step for many tasks in image registration techniques (Bhagalia et al. (2009)). The fundamental characteristic of any image registration technique is the type of spatial transformations or mapping used to properly overlay two images (Bolin & Huihui (2010)). This research uses affine transformation and scaling for comparison. Control point selection procedure in Matlab uses the code $cpselect(moving, fixed, movingpoints, fixedpoints)$. The results are displayed in form

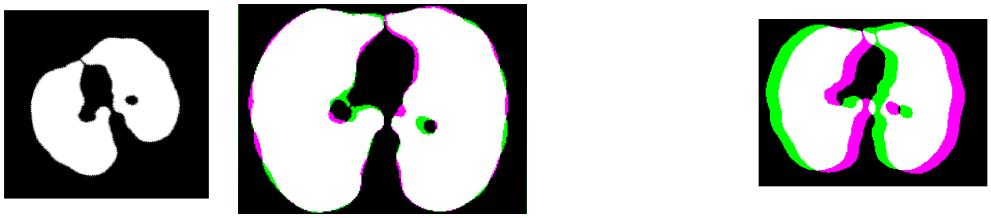

(a) Distorted Image02 (b) Adjusted Initial Radius02 (c) Registration Affine Image02 Model

Figure 3.4: Affine Registration for Image 02 with Adjusted Initial Radius.

(a) Distorted Image03 (b) Adjusted Initial Radius03 (c) Registration Affine Image03 Model

Figure 3.5: Affine Registration for Image 03 with Adjusted Initial Radius.

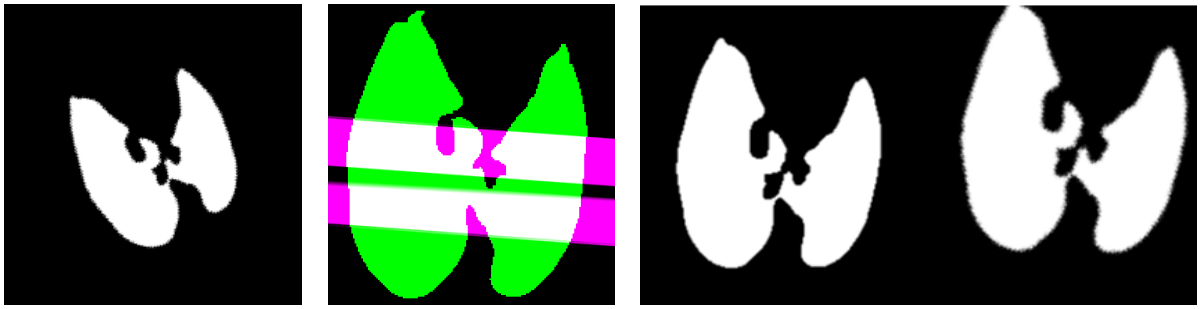

(a) Distorted Image04 (b) Registration using RSGD Image04 (c) Recovered Image04 Montage

Figure 3.6: RSGD Registration for Image 04 and its recovery.

(a) Fixed Image05 (b) Moving Image05 (c) Registration using RSGD Image05 Model (d) Registration using RSGD with 500 MI Image05 Model

Figure 3.7: RSGD Registration for Image 05.

of a matrix as follows:

$$\left[P_m\right] = \begin{bmatrix} 224.2500 & 223.2500 \\ 368.2500 & 150.7500 \\ 369.7500 & 238.2500 \\ 321.7500 & 245.2500 \\ 270.7500 & 251.7500 \\ 253.2500 & 134.2500 \\ 336.7500 & 134.2500 \\ 222.2500 & 166.2500 \end{bmatrix}$$

and

$$\left[P_f\right] = \begin{bmatrix} 228.0000 & 229.2500 \\ 355.5000 & 161.2500 \\ 369.5000 & 241.7500 \\ 321.5000 & 244.7500 \\ 272.0000 & 250.7500 \\ 253.5000 & 131.2500 \\ 340.5000 & 130.7500 \\ 227.5000 & 166.2500 \end{bmatrix}$$

3.3 Similarity Metric

Similarity measure is the second part of a registration process that computes the degree of alignment of the images. It can be categorised into two approaches, namely featured-based and voxel-based similarity measures. Feature-based approach requires a feature extraction step which can bring an error that can generally affect the registration algorithm and cannot be reversed later as suggested by Rueckert & Aljabar (2010). Voxel-based approach aims at determining the degree of similarity in the image intensities. Voxel similarity measures are generally preferred methods for measuring image similarity because they are robust and give better accuracy. According to Van der Bom et al. (2011), the three similarity measures that give good accuracy and robust results are gradient descent, gradient correlation and pattern intensity. The choice of the characteristic of the cost function and the search strategy as indicated by Klein et al. (2007), determines how successful the registration process becomes. Single modality image registration is best done using invariant moments while multi-modality image registration is best done using mutual information similarity measure. For images with rotational differences, cross correlation coefficients and invariant moments types of similarity measures are the best to apply. Mattes mutual information is the similarity metric used in this research.

3.3.1 Mean Squared Differences

In medical image registration techniques, accurate definition of similarity measures plays a very important role as pointed out by Ulysses & Conci (2010). The most commonly used intensity-based similarity metrics are mutual information, linear interpolation and mean squared differences. Mean Square Error (MSE), as shown by Peksinski et al. (2015), is a popular and commonly used medical image registration quality measure

which is expressed as follows:

$$MSE = \frac{\sum_{x=1}^{M} \sum_{y=1}^{N} [f_{in}(x,y) - f_{out}(x,y)]^2}{M.N}. \tag{3.6}$$

where $f_{in}(x,y)$ is original image; $f_{out}(x,y)$ is the registered image and $M.N$ is the resolution. The values for these images are also referred to as actual value for original image and predicted value for registered image. This metric has the advantage of being computationally simple and is based on the premise that pixels intensity in one image corresponds to pixels intensity in the second image.

3.3.2 Mutual Information

Mutual information between source and target images is used for determining visual quality. From information theoretic metrics, information fidelity criterion is bounded below by zero since mutual information can never be non negative, and bounded above by infinity which occurs when the source image is identical to the target image as indicated by Bovik (2009). Mutual information can be expressed as:

$$I(T,W) = \sum_{a} \sum_{b} P_{TW}(a,b) log \frac{P_{TW}(a,b)}{P_T(a) P_W(b)} \tag{3.7}$$

where,

T is a template, W is a window and both are random variables;

$P_T(a)$ is the probability that the intensity at a voxel in T is a and

$P_W(b)$ is the probability that the intensity at a voxel in W is b;

$P_{TW}(a,b)$ is the joint probability, which gives the probability that intensity a in the template lies on top of intensity b in the window.

In image registration using mutual information, the initial registration set-up involves

calling Image Processing Toolbox in Matlab. The two images to be registered are read onto Matlab workspace. If the input images are in colour, they are converted to gray scale from Red, Green and Blue (RGB). Depending on their dimensions, they can be scaled properly (resized) to less than 256 x 256 pixels. Translation, in-plane rotation and if necessary cropping are then carried out. Control points are selected on both the fixed and moving images then saved in the workspace. Geometric transformation is estimated using the $tform$ command in Matlab where the resultant output recovers scale and angle of rotation, theta. An optimiser is selected to minimise the cost function. Various properties of the optimiser such as the initial search radius and maximum iterations can be adjusted to improve the registration process. Successful registration is attained when optimisation converges to a local or global minimum. Below are results obtained for image registration using mutual information where the step value is fixed at 20 and there is no cropping.

Table 3.1: Calculation of Joint Entropy and Mutual Information

Image Pair	**Entropy 1**	**Entropy 2**	**Joint Entropy**	**Mutual Information**
01	691.2923	691.2923	1.5976	$1.3842 \times 10^{+3}$
02	673.9541	736.2445	2.0812	$1.4123 \times 10^{+3}$
03	726.5749	652.7596	1.8837	$1.3812 \times 10^{+3}$
04	948.3985	1013.9000	1.8383	$1.9641 \times 10^{+3}$
05	676.8840	610.7235	2.2973	$1.2899 \times 10^{+3}$
06	730.4745	777.7002	1.8288	$1.5100 \times 10^{+3}$

In tables 3.1-3.7 of image registration results, angle represents vector angle of rotation to check rotation, e.g. [-30:2:30] which is the same as angle=15, the step represents how many pixels to shift in the x and y directions to check translation, crop indicates if cropping needs to be performed or not, e.g. crop=0 means no cropping and crop=1 means crop part of the image and save computational time. Theta gives best angle of rotation, while I and J represent the coordinates to the top left corner of the matched

Table 3.2: Image Registration 01 using Mutual Information

Image	**Size**	**Theta**	**I**	**J**	θ	h_{min}	h_{max}
01F	$368 \times 418 \times uint8$	-2:1:2	2	1	-2	-2.3128	0
01M	$386 \times 462 \times uint8$	-8:4:8	2	1	-8	-2.3128	0
-	-	-10:2:10	2	1	-10	-2.3128	0
-	-	-10:5:10	2	1	-10	-2.3128	0
-	-	-20:4:20	2	1	-20	-2.3128	0
-	-	-20:5:20	2	1	-20	-2.3128	0
-	-	-30:3:30	2	1	-30	TME	TME
-	-	-30:5:30	2	1	-30	TME	TME
-	-	-30:10:30	2	1	-30	TME	TME

Table 3.3: Image Registration 02 using Mutual Information

Image	**Size**	**Theta**	**I**	**J**	θ	h_{min}	h_{max}
02F	$312 \times 420 \times uint8$	-2:1:2	1	41	2	-0.2739	0.1497
02M	$338 \times 462 \times uint8$	-8:4:8	1	41	8	-0.2739	0.1531
-	-	-10:2:10	1	41	8	-0.2739	0.1531
-	-	-10:5:10	1	61	10	-0.2739	0.1510
-	-	-20:4:20	1	61	-16	-0.2739	0.1581
-	-	-20:5:20	1	61	-15	-0.2739	0.1571
-	-	-20:10:20	1	61	20	-0.2739	0.1556
-	-	-30:3:30	61	81	30	-0.2739	0.1571
-	-	-30:5:30	61	81	30	-0.2739	0.1604
-	-	-30:10:30	61	81	30	-0.2739	0.1604

area of the large image as shown by Artyushkova et al. (2011). TME stands for too many elements.

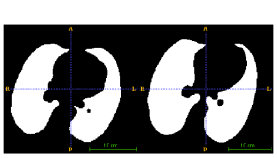

(a) Montage Image 01

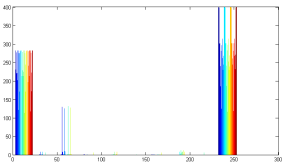

(b) Histogram Montage 01

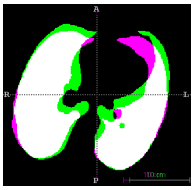

(c) Image 01 with 300 Maximum Iterations

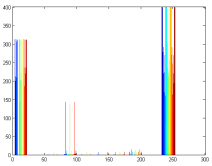

(d) Histogram Image 01 with 300 Maximum Iterations

Figure 3.8: Montage for Image 01 and its Histogram.

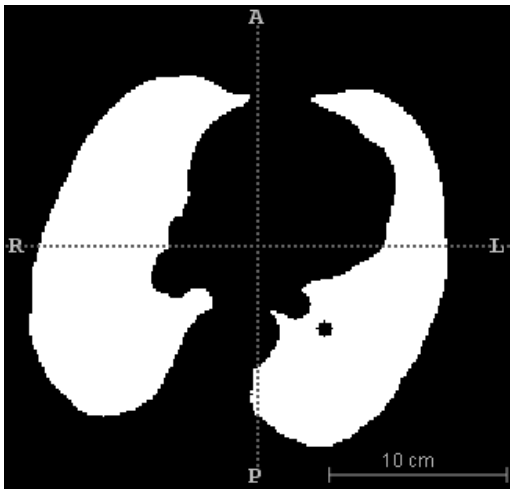

(a) Default Registration Image 01

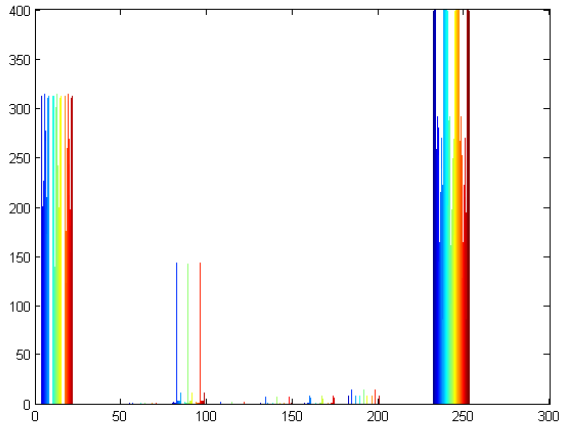

(b) Default Registration Histogram

Figure 3.9: Default Registration Image 01 and its Histogram..

Table 3.4: Image Registration 03 using Mutual Information

Image	**Size**	**Theta**	**I**	**J**	θ	h_{min}	h_{max}
03F	$296 \times 412 \times uint8$	-2:1:2	21	21	-2	0	0.5272
03M	$300 \times 434 \times uint8$	-8:4:8	21	21	-4	0	0.5860
-	-	-10:2:10	21	21	-4	0	0.5860
-	-	-10:5:10	21	21	-5	0	0.5882
-	-	-20:4:20	21	21	-4	0	0.5860
-	-	-20:5:20	21	21	-5	0	0.5882
-	-	-20:10:20	41	41	-10	0	0.5423
-	-	-30:3:30	21	21	-3	0	0.5655
-	-	-30:5:30	21	21	-5	0	0.5882
-	-	-30:10:30	41	41	-10	0	0.5423

Table 3.5: Image Registration 04 using Mutual Information

Image	**Size**	**Theta**	**I**	**J**	θ	h_{min}	h_{max}
04F	$432 \times 384 \times uint8$	-2:1:2	1	21	0	-19.1900	16.9927
04M	$436 \times 408 \times uint8$	-8:4:8	1	21	0	-19.1900	16.9927
-	-	-10:2:10	1	21	0	-19.1900	16.9927
-	-	-10:5:10	1	21	0	-19.1900	16.9927
-	-	-20:4:20	1	21	0	-19.1900	16.9927
-	-	-20:5:20	1	21	0	-19.1900	16.9927
-	-	-20:10:20	1	21	0	-19.1900	16.9927
-	-	-30:3:30	1	21	0	-19.1900	16.9927
-	-	-30:5:30	1	21	0	-19.1900	16.9927
-	-	-30:10:30	1	21	0	-19.1900	16.9927

Table 3.6: Image Registration 05 using Mutual Information

Image	**Size**	**Theta**	**I**	**J**	θ	h_{min}	h_{max}
05F	$282 \times 412 \times uint8$	-2:1:2	21	1	1	0	0.7211
05M	$294 \times 418 \times uint8$	-8:4:8	41	21	8	0	0.7213
-	-	-10:2:10	41	21	8	0	0.7213
-	-	-10:5:10	21	21	5	0	0.6862
-	-	-20:4:20	41	21	8	0	0.7213
-	-	-20:5:20	21	21	5	0	0.6862
-	-	-20:10:20	41	21	10	0	0.6617
-	-	-30:3:30	41	21	9	0	0.6924
-	-	-30:5:30	21	21	5	0	0.6862
-	-	-30:10:30	41	21	10	0	0.6617

Table 3.7: Image Registration 06 using Mutual Information

Image	**Size**	**Theta**	**I**	**J**	θ	h_{min}	h_{max}
06F	$318 \times 430 \times uint8$	-2:1:2	1	1	-1	0.1307	0.1604
06M	$318 \times 428 \times uint8$	-8:4:8	21	21	4	0	0.1575
-	-	-10:2:10	21	21	6	0	0.1706
-	-	-10:5:10	21	21	5	0	0.1745
-	-	-20:4:20	21	21	4	-0.0273	0.1575
-	-	-20:5:20	21	21	5	-0.0273	0.1745
-	-	-20:10:20	41	21	10	-0.0273	0.1292
-	-	-30:3:30	21	21	6	-0.1214	0.1706
-	-	-30:5:30	21	21	5	-0.1214	0.1745
-	-	-30:10:30	41	21	10	-0.1214	0.1292

3.4 Transformation

Estimation of transformation was carried out using function $tform$ to find fitting geometric transformation for moving points, P_m and fixed points, P_f. The function $tformInv$ was used to recover the scale and the angle of the rotated image. In order to create a geometric transformation object, the parameters of the geometric transformation need to be defined. The *imwarp* function performed the transformation by determining the values of pixels in the output image which are then mapped into new locations that correspond to similar locations in the input image. Table 3.8 shows details of recovered values of scale and angle theta for the three types of transformations, which are compared to the original. Results show that affine transformation gives the best results that are close to the original values, followed by projective transformation and the most divergent results were from non-reflective similarity transformation.

Table 3.8: Registered Image Recovery

Item	**Non-reflective Similarity**	**Affine**	**Projective**	**Original**
Scale Recovered	0.7764	0.6863	0.7553	0.7000
Theta Recovered	20.6824	29.7407	26.6684	30.0000

Table 3.9: Estimation Transformation

Similarity Transformation	**Moving Points**	**Fixed Points**	**Affine Values**
tform IR/3.5	0.9149	0.0000	0
”	0.0000	0.9149	0
”	4.4858	3.9777	1.0000
tform IR/4.0	0.9147	0.0000	0
”	0.0000	0.9147	0
”	4.6593	5.0475	1.0000
tform IR/6.0	0.9224	0.0000	0
”	0.0000	0.9224	0
”	1.3062	2.4753	1.0000

3.5 Optimisation Techniques

The last component of image registration algorithm is the optimisation process, whose tools define the process for minimising or maximising the similarity measure. Optimisation process iteratively minimises the cost function and updates parameters during image registration framework. A dependable optimiser will reliably and quickly find the best possible transformation. Registration via optimisation is a variational-based approach as demonstrated by Matjelo et al. (2015), which allows a sound mathematical treatment, characterisation, formulation as well as classification of some of the most commonly used procedures. A search algorithm greatly contributes to the accuracy of a registration procedure. In this research, Regular Step Gradient Descent (RSGD) optimisation algorithm is used to minimise the cost function. The convergence property values of RSGD such as the growth factor in search radius, initial radius, epsilon and maximum iterations are changed to give varying results. Optimisation parameters such as minimum step length, the relaxation factor, the initial step length and number of iterations are defined. The minimum step length and the number of iterations act as the stopping criteria for the optimisation.

Optimisation algorithms used for formulation of engineering design problems vary from problem to problem. Not a single algorithm can work for all optimisation problems efficiently and accurately. Optimisation algorithms are classified into two categories, namely: direct methods and gradient-based methods. The difference between the two is that direct methods do not use any derivative information of the cost function while gradient-based methods require the first and/or the second order derivative information of the cost function to guide the search process. Most optimisation algorithms employ the following iterative scheme:

$$p_{k+1} = p_k + a_k d_k \tag{3.8}$$

where a_k is scalar gain factor and d_k search direction.

Choice of the gain sequence is critical to the performance of the optimisation strategy. Depending on the strategy adopted, it can be determined as follows:

1. As a constant where $a_k = a$

2. Slowly decaying:

$$a_k = f(k) = \frac{a}{(A+k)^{\alpha}} \tag{3.9}$$

where α governs the decay rate and A is the stability constant.

When the term α=1, this becomes the condition for theoretically optimal setting rate of convergence as shown by Qiao et al. (2016). When k=0, the gain function is at maximum $a_0 = \frac{a}{(A)}$ and the sigmoid function $f(0) = 0$, out of which:

$$f(k) = \frac{f_{max} - f_{min}}{1 - (\frac{f_{max}}{f_{min}})e^{\frac{-k}{\omega}}} + f_{min} \tag{3.10}$$

where f_{max} determines the maximum gain at each iteration, f_{min} indicates the maximal step backward in time and ω affects the shape of the sigmoid function. Convergence is achievable when $k \geq 0$ and the maximum of the sigmoid function when $f_{max} = 1$ as shown by Qiao et al. (2016) and Klein et al. (2009). From the above equation, it can be observed that asymptotic normality and convergence can be assured when $f_{max} > -f_{min}$ and $\omega > 0$.

3. As an exact line search:

$$a_k = argmin_a C(p_k + ad_k) \tag{3.11}$$

4. As inexact line search:

$$a_k \approx argmin_a C(p_k + ad_k) \tag{3.12}$$

5. As adaptive:

$$a_k = F(progress\, from\, previous\, iterations) \tag{3.13}$$

The performance of an optimisation algorithm depends very much on the choice of the gain sequence. Parameters such as the α, that govern the decay rate are chosen within the range $0 < \alpha \leq 1$. To take advantage of asymptotic optimality, it is beneficial to convert $\alpha = 1$ and $\gamma = \frac{1}{6}$ if the algorithm runs a large number of iterations. Typical practical values for these parameters are $\alpha = 0.602$ and $\gamma = 0.101$ in the equations:

$$a_k = \frac{a}{(A + k)^\alpha}$$

$$c_k = \frac{c}{(k + 1)^\gamma}$$

where a, c, A are non-negative coefficients.

Chosen values of a, A are done at the same time to attain a good performance of the optimisation algorithm where $A > 0$ and $a_0 = \frac{a}{(1 + A)^{0.602}}$.
For regular step gradient descent optimiser configuration, the following properties are taken into consideration:

1. Gradient magnitude tolerance which is a positive scalar value that controls the optimisation process;

2. Minimum step length which is a positive scalar that controls the accuracy of convergence;

3. Maximum step length which is a positive scalar that controls the initial step length used in optimisation, whose default value is 0.0625;

4. Maximum number of iterations which is a positive scalar integer that determines the maximum number of iterations the optimiser performs at any given pyramidal level;

5. Relaxation factor, also referred to as step length reduction factor which is a scalar value between 0 and 1 that defines the rate at which the optimiser reduces the step sizes during convergence. It has a default value of 0.5.

Choosing the $\alpha < 1$ makes the step size to decay less faster. When a is set too small, the optimisation method suffers from slow convergence and a large a may cause the process to become unstable. Convergence analysis for iterative systems' stability and speed is comprehensively discussed by Berenguer-Vidal et al. (2015).

3.5.1 Regular Step Gradient Descent Optimisation

Optimisation-based registration requires that a similarity or dissimilarity measure is defined, initial parameters that nearly register the images are found and an algorithm is developed to run the initial registration to completion as discussed by Goshtasby (2012). To use regular step gradient descent optimiser, the following steps are carried out:

Step 1: Create a *regularstepgradientdescent* object to register a set of lung CT scan images;

Step 2: Create suitable optimisation configuration object for registering the two images;

Step 3: Create a metric configuration object;

Step 4: Modify the optimiser object to acquire more precision;

Step 5: Perform registration;

(a) Image 01 RSGD registered (b) Image 02 RSGD registered (c) Image 03 RSGD registered

Figure 3.10: RSGD Registered Images 01-03.

(a) Image 04 RSGD registered (b) Image 05 RSGD registered (c) Image 06 RSGD registered

Figure 3.11: RSGD Registered Images 04-06.

Step 6: View the registered images.

In Figure 3.10 and 3.11, we show images of lung CT scans registered using RSGD optimisation algorithm.

3.5.2 One to One Evolutionary Optimisation

One to one evolutionary optimisation algorithm is one of the simplest yet very powerful Evolutionary Strategies (ES). It is usually denoted by (1+1)-ES as given by (Sbalzarini 2000). The simple idea in evolutionary algorithms is to imitate the natural biological process to solve the optimisation problem described using a limited number of parameters. Evolutionary algorithm as discussed by Eiben & Smith (2003) has the underlying

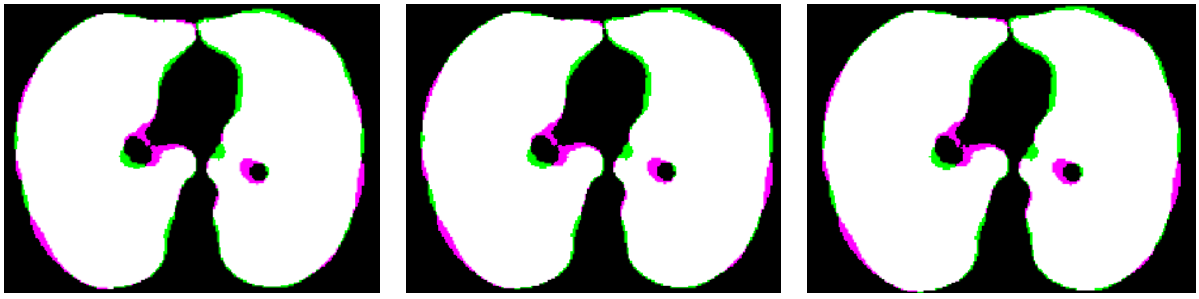

(a) Adjusted Initial Radius Image 02 with a Maximum Iteration 500

(b) Adjusted Initial Radius Image 02 with a Maximum Iteration 800

(c) Adjusted Initial Radius Image 02 with a Maximum Iteration 1000

Figure 3.12: Registration with Adjusted Initial Radius for Image 02 and various Maximum Iteration.

(a) Adjusted Initial Radius Image 03 with a Maximum Iteration 500

(b) Adjusted Initial Radius Image 03 with a Maximum Iteration 800

(c) Adjusted Initial Radius Image 03 with a Maximum Iteration 1000

Figure 3.13: Registration with Adjusted Initial Radius for Image 03 with various Maximum Iteration.

principle that given a population of individuals, the surrounding conditions cause natural selection which results in fitness in the population (survival for the fittest). A group of different parameter vectors is created and named a population of individuals. This produces a population size. The quantity and quality of these parameter vectors describe a scalar valued fitness function also referred to as cost function. If the aim of the optimisation is to minimise (maximise) the cost function, then parameter vectors with lower (greater) fitness value are considered better respectively.

One to one evolutionary optimisation algorithm generates a random sample as shown by Eikvil et al. (2005) around the current posistion in the parametric space. They perform better than gradient descent type optimisers when the metrics are noisy. Evolutionary Optimisation (EO) principles presented by Deb (2011) differ from typical optimisation algorithms in that their procedures do not use gradient information in their search process. This means that they are direct search methodologies which allow them to be used in a wide variety of optimisation problems. EO use a population approach in an iteration unlike the typical optimisation algorithm which uses a point approach. The advantages of a population approach include quick computational search, finds multiple optimal solutions and has the ability to normalise decision variables as suggested by Deb (2011). EO uses stochastic operators as opposed to the typical optimisation algorithms that use deterministic operators. Evolutionary algorithm model discussed by Mwaura & Keedwell (2010) are based on stochastic algorithms and follow the listed down steps as a general methodology for solutions to population based EA problems:

Step 1: Create an initial population of solutions $P(0) = (P_1(0), ..., P_n(0))$;

Step 2: Compute the fitness $f(P_i(t))$, for each individual $P_i(t)$, of the current population $P(t)$. $P_i(t)$ refers to an individual i in $P(t)$ and t is the number of generations;

Step 3: Select parent organism by applying selection method and/or replication;

Step 4: Apply genetic operations on parent individuals to create offspring $P(t+1)$ that

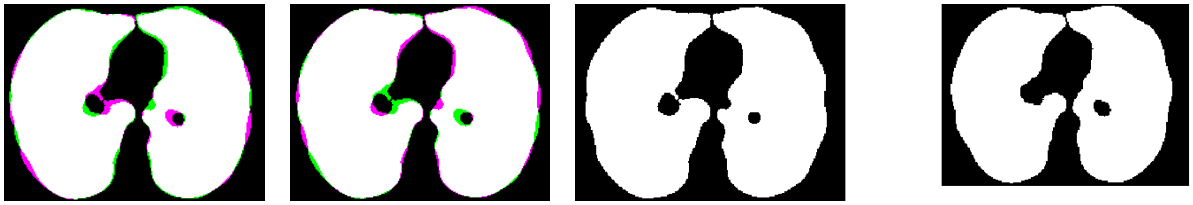

(a) Registration by 1+1 ES Image02 (b) Registration by RSGD Image02 (c) Unregistered Montage Image02

Figure 3.14: Registration using ES for Image 02.

make up the next generation or replace individuals in the current population and

Step 5: Go to step 2; if maximum fitness has been achieved or maximum generation attained exit algorithm else go to step 3.

3.6 Performance Evaluation

Expert judgement method for performance evaluation of image registration provided better visual perception, quicker user recognition and interaction as suggested by Coutre et al. (2000). Colour enhanced images assist in visualisation. Visualisation brings together human perception and cognitive ability to provide analysis on image registration. Expert judgement is applied to evaluate registration performance by scoring the colour enhanced images based on quality. Acquisition and application of NUMERICS software shown by Gerganov et al. (2012b) would also prove useful in validation of the registration algorithm used. During qualitative and quantitative validation of image registration, Target Registration Error (TRE) is calculated as shown by Yin et al. (2009). Different performance evaluation measures are applied depending on expertise of registration. Such measures include image intensity-based metrics where Root Mean Square (RMS) as indicated by Yan et al. (2012), Median Absolute Deviation (MAD) and Maximum Intensity Differences (MID) are calculated according to Yin et al. (2009). The other

method is where expert review is employed, based on anatomical landmarks.

CHAPTER 4. ANALYSIS AND DISCUSSION OF RESULTS

4.1 Similarity Metric

Several lung CT scan pairs from EMPIRE 10 data set were registered using mutual information similarity metric and affine transformation where the metrics were subjected to two optimisers, RSGD and EO in order to minimise the cost function and achieve the required convergence. The results are compared both quantitatively and qualitatively to check on quality measure. Table 3.1 shows the results of calculation of joint entropy and mutual information for each set of lung CT scans. Mutual information calculated is the Shannon type which is a powerful measure of similarity between multi-modality images being registered. It is given by the difference between the sum of Shannon's marginal entropies and the joint entropy. Mutual information depends on relative occurrence in each of the images separately and the combined co-occurrence in both images, which explains Eq (2.13). Joint entropy results for CT scan pairs 02 and 05 images are very similar, and their values are 2.0812 and 2.2973 respectively, as shown in Table 3.1. CT scan pairs 03, 04 and 06 similarly have their joint entropy values in the range of 1.82-1.88. These results give an indication of quality measure for the selected metric. Results of Tables 3.2-3.7 give values of minimum (h_{min}) and maximum (h_{max}) mutual information, theta (the best angle of rotation), I and J (coordinates of top left corner of the matched area of image being mapped on) as outputs during calculation of mutual information. The work of Han (2010) presented feature-constrained lung CT registration

using mutual information and stochastic gradient descent optimisation scheme, whose results on correspondence of annotated point pairs compares well with our results. Fig. 3.10 shows registered lung CT scan images when mutual information was used to evaluate alignment of the two pairs of images. The alignment has been driven by choosing the overlap with large marginal entropies. The overlap has equal area of foreground and background intensities represented by green and magenta for fixed and moving images respectively. The white portion shows area of common intensities.

4.2 Transformation

From the results of Table 3.8, it was observed by fitting transformation to the control points, affine transformation produced the best recovered image when compared to both non-reflective similarity and projective transformations. Affine transformation gave the closest values to the original image for both the scale and the angle.

4.3 Optimisation

The following two optimisation algorithms were chosen to minimise the objective function:

1 : Regular Step Gradient Descent

2 : One to One Evolutionary

4.3.1 Regular Step Gradient Descent

Fig. 3.1-3.3 show lung CT scans for all the six data sets registered using regular step gradient descent optimisation algorithm. The Moving Image 01 in Fig. 3.1 b) appears

that way because it was very dark. Fig. 3.4 shows Affine Registration for Image 02 with adjusted initial radius. The distorted image is displayed in Fig. 3.4 a), after performing initial radius adjustment for image 02, the results shown in Fig. 3.4 b) and the overall results of registration using affine transformation are contained in Fig. 3.4 c). These results show an overlap with slightly wider borderline indicated by the green and magenta colours. The centre white shows areas of common intensity. Fig. 3.5 a)-c) show registration for Image 03 using the same process. Registration for Image 04 using RSGD optimisation and its recovered montage are shown in Fig. 3.6. It was observed that the registration of the image sets was well aligned with very impressive results. This tallies well with the results shown in Table 3.8. The fixed and moving images for CT scan 05 are shown in Fig. 3.7 a) and b). Registration results for Image 05 using RSGD optimisation and Maximum Iteration (MI) at a value of 500 are shown in Fig. 3.7 c) and d). Fig 3.8 a)and b) show results of montage Image 01 and the generated histogram respectively. Image 01 with MI of 300 is shown in Fig. 3.8 c) and its generated histogram in Fig. 3.8 d). Default registration Image 01 and its generated histogram are shown in Fig. 3.9 a) and b) respectively. Fig. 3.11 gives results for registered Images 01-06 using regular step gradient descent optimisation algorithm. When certain properties of the optimiser have been changed, the registered images showed little or no effect. The initial radius was reduced by a factor of 3.5, kept constant and the maximum iterations were varied from 100, 500, 800 and 1000. Fig 3.12 shows results for data set of Image 02 but similar results were found for all the other data sets. It was noted that change in maximum iterations had little or no effect on the resultant registered image. This was observed from Fig. 3.13 where three images for Image 03 with adjusted radius and different values for maximum iterations were registered.

4.3.2 One to One Evolutionary

Fig. 3.14 gives the results of the two optimisation algorithms. In the results for one plus one evolutionary method, shown in Fig. 3.14 a), the registered image showed overlap of magenta over green. In the results of regular step gradient descent method, shown in Fig. 3.14 b), the registered image showed overlap of green over magenta. The results presented here are for Image 02 but they are the same for the rest of the Images 03-06. Both optimisation methods have similar results, the difference being the interchange of overlap areas. The areas of common intensity remain the same for all registered images.

CHAPTER 5. CONCLUSION AND RECOMMENDATIONS

5.1 Conclusion

In this research, several image registration techniques were discussed. However, image registration using affine transformation, mutual information as the similarity measure, linear interpolation, RSGD and EO as optimisation algorithms were investigated. Image registration is a wide field of research that develops mathematical algorithms to analyse information from medical images, satellite images, remote sensing equipment, etc. for use in various applications, such as clinical and basic scientific research. The algorithms and mathematical models developed assist in finding solutions to specific engineering problems. Image registration of lung CT scans was successfully performed. The results compared well with documented results from EMPIRE 10 Challenge research, especially where landmark matching were investigated. Affine transformation was applied in this research but it is possible to include non-rigid transformations like B-Splines or Thin-Plate Splines transforms. Where such cases occur, Principal Component Analysis (PCA) will be employed because many more parameters need to be trained. Mutual information is a distinctive similarity measure particularly for multi-modal medical imaging registration techniques. They have been shown to be robust to occlusions and illumination intensity variations making them good for alignment. The results of this research conforms to both theoretical principles as well as practical applications. Therefore, the contribution of this research is its potential to increase the scientific understanding of

image registration of anatomical body organs and it lays a basis for future research in performance evaluation of registration techniques.

5.2 Recommendations

1. Further research using Artificial Neural Networks (ANN) for transformation parameter validation and big data handling would be an important area to deal with.

2. Detailed experiments with different similarity measures and different optimisers would shed more light in the knowledge area of image registration not only for medical images but also other fields like remote sensing, Geographic Information System (GIS), satellite communication and mapping, biomedical engineering, robotics and so forth.

3. There is need to carry out a further research with additional data sets in order to validate the applicability of the procedures to other types of algorithms and application areas.

Bibliography

Adler D.H. 2011. *Accelerated Medical Image Registration using the Graphics Processing Unit*. Ph.D. thesis, UNIVERSITY OF CALGARY.

Arguillère S., Miller M., & Younes L. 2015. Lddmm surface registration with atrophy constraints. *arXiv preprint arXiv:1503.00765*.

Artyushkova K., Fenton J., Farrar J., & Fulghum J.E. 2011. Multitechnique fusion of imaging data for heterogeneous materials. *image*, 200(700):x700μm.

Baudin M., Couvert V., & Steer S. 2010. Optimization in scilab. Technical report, Technical report, Scilab Consortium, July 2010. http://forge. scilab. org/index. php/p/docoptimscilab.

Berenguer-Vidal R., Verdú-Monedero R., & Morales-Sánchez J. 2015. Convergence analysis of multidimensional parametric deformable models. *Computer Vision and Image Understanding*, 135:157–177.

Bhagalia R., Fessler J.A., & Kim B. 2009. Accelerated nonrigid intensity-based image registration using importance sampling. *Medical Imaging, IEEE Transactions on*, 28(8):1208–1216.

Blomgren P. 2014. Numerical optimization. *Convergence*.

Bolin F. & Huihui T. 2010. Image registration based on thin plate spline non-rigid medical. *Comput. Simul*, 27:275–278.

Bovik A.C. 2009. *The essential guide to image processing.* Academic Press.

Boyd S. & Vandenberghe L. 2009. *Convex optimization.* Cambridge university press.

Brooks R. & Arbel T. 2007. Improvements to the itk:: Kerneltransform and subclasses. *Insight J.*

Bunting P., Labrosse F., & Lucas R. 2010. A multi-resolution area-based technique for automatic multi-modal image registration. *Image and Vision Computing*, 28(8):1203–1219.

Byrd R.H., Hansen S., Nocedal J., & Singer Y. 2014. A stochastic quasi-newton method for large-scale optimization. *arXiv preprint arXiv:1401.7020*.

Castillo R., Castillo E., Fuentes D., Ahmad M., Wood A.M., Ludwig M.S., & Guerrero T. 2013. A reference dataset for deformable image registration spatial accuracy evaluation using the copdgene study archive. *Physics in medicine and biology*, 58(9):2861.

Ceritoglu C., Wang L., Selemon L.D., Csernansky J.G., Miller M.I., & Ratnanather J.T. 2010. Large deformation diffeomorphic metric mapping registration of reconstructed 3d histological section images and in vivo mr images. *Frontiers in human neuroscience*, 4.

Chen C.h. 2010. *Stochastic simulation optimization: an optimal computing budget allocation*, volume 1. World scientific.

Chen H.F. 2003. Stochastic approximation algorithms with expanding truncations. *Stochastic Approximation and Its Applications*, 25–93.

Coutre S.C., Evens M., & Armato S. 2000. Performance evaluation of image registration. In *Engineering in Medicine and Biology Society, 2000. Proceedings of the 22nd Annual International Conference of the IEEE*, volume 4, 3140–3143. IEEE.

Dasgupta B., Divya K., Mehta V.K., & Deb K. 2013. Repamo: Recursive perturbation approach for multimodal optimization. *Engineering Optimization*, 45(9):1073–1090.

de Groot M., Vernooij M.W., Klein S., Ikram M.A., Vos F.M., Smith S.M., Niessen W.J., & Andersson J.L. 2013. Improving alignment in tract-based spatial statistics: Evaluation and optimization of image registration. *NeuroImage*, 76:400–411.

Deb K. 2011. Multi-objective optimisation using evolutionary algorithms: an introduction. In *Multi-objective evolutionary optimisation for product design and manufacturing*, 3–34. Springer.

Delibasis K., Asvestas P.A., & Matsopoulos G.K. 2010. Multimodal genetic algorithms-based algorithm for automatic point correspondence. *Pattern Recognition*, 43(12):4011–4027.

Delibasis K.K., Asvestas P.A., & Matsopoulos G.K. 2011. Automatic point correspondence using an artificial immune system optimization technique for medical image registration. *computerized medical imaging and graphics*, 35(1):31–41.

Deshmukh M. & Bhosle U. 2011. A survey of image registration. *International Journal of Image Processing (IJIP)*, 5(3):245.

Ding L., Goshtasby A., & Satter M. 2001. Volume image registration by template matching. *Image and Vision Computing*, 19(12):821–832.

Doi K. 2007. Computer-aided diagnosis in medical imaging: historical review, current status and future potential. *Computerized medical imaging and graphics*, 31(4):198–211.

Dura E., Domingo J., Ayala G., & Martí-Bonmatí L. 2012. Evaluation of the registration of temporal series of contrast-enhanced perfusion magnetic resonance 3d images of the liver. *Computer methods and programs in biomedicine*, 108(3):932–945.

Eiben A.E. & Smith J.E. 2003. *Introduction to evolutionary computing*, volume 53. Springer.

Eikvil L., Husøy P.O., & Ciarlo A. 2005. Adaptive image registration. In *Proceedings of ESA-EUSC 2005 workshop on Image Information mining–Theory and Application to Earth observation*, 5–7.

Ezzeldeen R., Ramadan H., Nazmy T., Yehia M.A., & Abdel-Wahab M. 2010. Comparative study for image registration techniques of remote sensing images. *The Egyptian Journal of Remote Sensing and Space Science*, 13(1):31–36.

Ferrante E. & Paragios N. 2013. Non-rigid 2d-3d medical image registration using markov random fields. In *Medical Image Computing and Computer-Assisted Intervention–MICCAI 2013*, 163–170. Springer.

Fischer B. & Modersitzki J. 2008. Ill-posed medicine-an introduction to image registration. *Inverse Problems*, 24(3):034008.

Fitzpatrick J.M., Hill D.L., & Maurer Jr C.R. 2000. Image registration. *Handbook of medical imaging*, 2:447–513.

Floca R. & Dickhaus H. 2007. A flexible registration and evaluation engine (free). *Computer methods and programs in biomedicine*, 87(2):81–92.

Fluck O., Vetter C., Wein W., Kamen A., Preim B., & Westermann R. 2011. A survey of medical image registration on graphics hardware. *Computer methods and programs in biomedicine*, 104(3):e45–e57.

Gerganov G., Kawrakow I., Kuvandjiev V., Dimitrova I., & Mitev K. 2012a. Performance evaluation of 2d image registration algorithms with the numerics image registration and comparison platform. In *EUROPEAN MEDICAL PHYSICS AND ENGINEERING CONFERENCE*.

Gerganov G., Kuvandjiev V., Dimitrova I., Kawrakow I., & Mitev K. 2012b. Numerics: An online image registration and image comparison platform. In *Nuclear Science Symposium and Medical Imaging Conference (NSS/MIC), 2012 IEEE*, 3930–3935. IEEE.

Glocker B.M. et al. 2011. *Random Fields for Image Registration*. München, Technische Universität München, Diss., 2011.

Goshtasby A.A. 2012. *Image registration: Principles, tools and methods*. Springer Science & Business Media.

Gupta A., Verma H.K., & Gupta S. 2012. Technology and research developments in carotid image registration. *Biomedical Signal Processing and Control*, 7(6):560–570.

Han X. 2010. Feature-constrained nonlinear registration of lung ct images. *Medical image analysis for the clinic: a grand challenge*, 63–72.

Hauser K. 2012. Document b553. *Gradient Descent, January*, 24.

Heger D. 2014. Big data analyticswhere to go from here. *International Journal of Develkopments in Big Data and Analytics*, 1(1):42–58.

Heinrich M.P., Jenkinson M., Bhushan M., Matin T., Gleeson F.V., Brady M., & Schnabel J.A. 2012. Mind: Modality independent neighbourhood descriptor for multi-modal deformable registration. *Medical Image Analysis*, 16(7):1423–1435.

Hennig P. & Kiefel M. 2013. Quasi-newton methods: A new direction. *The Journal of Machine Learning Research*, 14(1):843–865.

Hopp T., Dietzel M., Baltzer P.A., Kreisel P., Kaiser W.A., Gemmeke H., & Ruiter N.V. 2013. Automatic multimodal 2d/3d breast image registration using biomechanical fem models and intensity-based optimization. *Medical image analysis*, 17(2):209–218.

Jiang J., Trundle P., & Ren J. 2010. Medical image analysis with artificial neural networks. *Computerized Medical Imaging and Graphics*, 34(8):617–631.

Kabus S., Netsch T., Fischer B., & Modersitzki J. 2004. B-spline registration of 3d images with levenberg-marquardt optimization. In *Medical Imaging 2004*, 304–313. International Society for Optics and Photonics.

Klein S. 2008. *Optimisation methods for medical image registration*. PhD thesis, Image Sciences Institute, UMC Utrecht.

Klein S., Pluim J.P., Staring M., & Viergever M.A. 2009. Adaptive stochastic gradient descent optimisation for image registration. *International journal of computer vision*, 81(3):227–239.

Klein S., Staring M., Andersson P., & Pluim J.P. 2011. Preconditioned stochastic gradient descent optimisation for monomodal image registration. In *Medical Image Computing and Computer-Assisted Intervention–MICCAI 2011*, 549–556. Springer.

Klein S., Staring M., Murphy K., Viergever M.A., & Pluim J.P. 2010. Elastix: a toolbox for intensity-based medical image registration. *Medical Imaging, IEEE Transactions on*, 29(1):196–205.

Klein S., Staring M., & Pluim J.P. 2006. A comparison of acceleration techniques for nonrigid medical image registration. In *Biomedical Image Registration*, 151–159. Springer.

Klein S., Staring M., & Pluim J.P. 2007. Evaluation of optimization methods for nonrigid medical image registration using mutual information and b-splines. *Image Processing, IEEE Transactions on*, 16(12):2879–2890.

Kosiński W., Michalak P., & Gut P. 2012. Robust image registration based on mutual information measure. *Journal of Signal and Information Processing*, 3:175.

Kramer O. 2014. *A Brief Introduction to Continuous Evolutionary Optimization*. Springer.

Lee J.D., Sun Y., & Saunders M.A. 2014. Proximal newton-type methods for minimizing composite functions. *SIAM Journal on Optimization*, 24(3):1420–1443.

Levy Y. & Ellis T.J. 2006. A systems approach to conduct an effective literature review in support of information systems research. *Informing Science: International Journal of an Emerging Transdiscipline*, 9(1):181–212.

Lewis A.S. & Overton M.L. 2013. Nonsmooth optimization via quasi-newton methods. *Mathematical Programming*, 141(1-2):135–163.

Lombaert H., Grady L., Pennec X., Peyrat J.M., Ayache N., & Cheriet F. 2013. Groupwise spectral log-demons framework for atlas construction. In *Medical Computer Vision. Recognition Techniques and Applications in Medical Imaging*, 11–19. Springer.

Lu X., Ma H., & Zhang B. 2012. A non-rigid medical image registration method based on improved linear elastic model. *Optik-International Journal for Light and Electron Optics*, 123(20):1867–1873.

Machowski L.A. & Marwala T. 2007. Evolutionary optimisation methods for template based image registration. *arXiv preprint arXiv:0705.1674*.

Markelj P., Tomaževič D., Likar B., & Pernuš F. 2012. A review of 3d/2d registration methods for image-guided interventions. *Medical image analysis*, 16(3):642–661.

Matjelo N.J., Nicolls F., & Muller N. 2015. Evaluation of optimal control-based deformable registration model. In *New Trends in Networking, Computing, E-learning, Systems Sciences, and Engineering*, 117–124. Springer.

Menon M.H.P. & Narayanankutty K. 2010. Applicability of non-rigid medical image registration using moving least squares. *International Journal of Computer Applications*, 1(6):85–92.

Meskine F., Taleb N., El-Mezouar M.C., Kpalma K., Almhdie A., et al. 2013. A rigid point set registration of remote sensing images based on genetic algorithms & hausdorff distance. *World Academy of Science, Engineering and Technology*, 1095–1100.

Modat M., McClelland J., & Ourselin S. 2010. Lung registration using the niftyreg package. *Medical Image Analysis for the Clinic-A Grand Challenge*, 33–42.

Murphy K., van Ginneken B., Schilham A.M., De Hoop B., Gietema H., & Prokop M. 2009. A large-scale evaluation of automatic pulmonary nodule detection in chest ct using local image features and k-nearest-neighbour classification. *Medical Image Analysis*, 13(5):757–770.

Mwaura J. & Keedwell E. 2010. Evolution of robotic behaviours using gene expression programming. In *IEEE congress on Evolutionary Computation*, 1–8. IEEE.

Pai A., Sommer S., Darkner S., Sørensen L., Sporring J., & Nielsen M. 2014. Stepwise inverse consistent eulers scheme for diffeomorphic image registration. In *Biomedical Image Registration*, 223–230. Springer.

Paquin D. 2007. *Multiscale Methods for Image Registration*. Ph.D. thesis, Stanford University.

Peksinski J., Mikolajczak G., & Kowalski J. 2015. Peak mean square error indicator biometric analysis in the study of fingerprints. In *Environmental Science and Information Application Technology: Proceedings of the 2014 5th International Conference on Environmental Science and Information Application Technology (ESIAT 2014), Hong Kong, November 7-8, 2014*, 15. CRC Press.

Plakhov A. & Cruz P. 2004. A stochastic approximation algorithm with step-size adaptation. *Journal of Mathematical Sciences*, 120(1):964–973.

Qiao Y., van Lew B., Lelieveldt B.P., & Staring M. 2016. Fast automatic step size estimation for gradient descent optimization of image registration. *IEEE transactions on medical imaging*, 35(2):391–403.

Qiu Z., Tang H., & Tian D. 2009. Non-rigid medical image registration based on the thin-plate spline algorithm. In *Computer Science and Information Engineering, 2009 WRI World Congress on*, volume 2, 522–527. IEEE.

Ramírez-Quintana J.A., Chacon-Murguia M.I., & Chacon-Hinojos J.F. 2012. Artificial neural image processing applications: A survey. *Engineering Letters*, 20(1).

Rao S.S. & Rao S. 2009. *Engineering optimization: theory and practice*. John Wiley & Sons.

Risser L., Vialard F.X., Murgasova M., Holm D., & Rueckert D. 2010. Large deformation diffeomorphic registration using fine and coarse strategies. In *Biomedical Image Registration*, 186–197. Springer.

Rueckert D. & Aljabar P. 2010. Nonrigid registration of medical images: Theory, methods, and applications [applications corner]. *Signal Processing Magazine, IEEE*, 27(4):113–119.

Schreibmann E., Thorndyke B., Li T., Wang J., & Xing L. 2008. Four-dimensional image registration for image-guided radiotherapy. *International Journal of Radiation Oncology* Biology* Physics*, 71(2):578–586.

Shi Z. & He L. 2010. Application of neural networks in medical image processing. In *Proceedings of the second international symposium on networking and network security*, 2–4.

Sotiras A., Davatzikos C., & Paragios N. 2013. Deformable medical image registration: A survey. *Medical Imaging, IEEE Transactions on*, 32(7):1153–1190.

Ulysses J. & Conci A. 2010. Measuring similarity in medical registration. In *IWSSIP 17th International Conference on Systems, Signals and Image Processing*.

Valsecchi A., Damas S., & Santamaría J. 2012. An image registration approach using genetic algorithms. In *Evolutionary Computation (CEC), 2012 IEEE Congress on*, 1–8. IEEE.

Van der Bom I., Klein S., Staring M., Homan R., Bartels L., & Pluim J. 2011. Evaluation of optimization methods for intensity-based 2d-3d registration in

x-ray guided interventions. In *SPIE Medical Imaging*, 796223–796223. International Society for Optics and Photonics.

Vujović I. 2015. Multiresolution approaches in image processing. In *Multiresolution Approach to Processing Images for Different Applications*, 5–9. Springer.

Wang J., Brown M.S., & Tan C.L. 2009. Automatic corresponding control points selection for historical document image registration. In *2009 10th International Conference on Document Analysis and Recognition*, 1176–1180. IEEE.

Wang X.Y., Feng D.D., & Jin J. 2001. Elastic medical image registration based on image intensity. In *Proceedings of the Pan-Sydney area workshop on Visual information processing-Volume 11*, 139–142. Australian Computer Society, Inc.

Wu J. & Murphy M.J. 2010. Assessing the intrinsic precision of 3d/3d rigid image registration results for patient setup in the absence of a ground truth. *Medical physics*, 37(6):2501–2508.

Wyawahare M.V., Patil P.M., Abhyankar H.K., et al. 2009. Image registration techniques: an overview. *International Journal of Signal Processing, Image Processing and Pattern Recognition*, 2(3):11–28.

Yaegashi Y., Tateoka K., Fujimoto K., Nakazawa T., Nakata A., Saito Y., Abe T., Yano M., & Sakata K. 2013. Assessment of similarity measures for accurate deformable image registration. *Journal of Nuclear Medicine & Radiation Therapy*, 2012.

Yan L., Liu Y., Xiao B., Xia Y., & Fu M. 2012. A quantitative performance evaluation index for image fusion: Normalized perception mutual information. In *Control Conference (CCC), 2012 31st Chinese*, 3783–3788. IEEE.

Yin L., Tang L., Hamarneh G., Celler A., Shcherbinin S., Fua T., Carolan H., Thompson A., Liu M., & Duzenli C. 2009. Evaluating geometrical accuracy of image registration methods in spect guided radiation therapy. In *Medical Image Computing and Computer-Assisted Intervention Workshop on Geometric accuracy in image guided intervention (MICCAI GAIGI)*, 63–70.

Zhang Q. & Li H. 2007. Moea/d: A multiobjective evolutionary algorithm based on decomposition. *Evolutionary Computation, IEEE Transactions on*, 11(6):712–731.

Zhigljavsky A. & Žilinskas A. 2007. *Stochastic global optimization*. Springer.

Zikic D., Glocker B., Kutter O., Groher M., Komodakis N., Khamene A., Paragios N., & Navab N. 2010. Markov random field optimization for intensity-based 2d-3d registration. In *SPIE Medical Imaging*, 762334–762334. International Society for Optics and Photonics.

Zitova B. & Flusser J. 2003. Image registration methods: a survey. *Image and vision computing*, 21(11):977–1000.

APPENDIX A. Proof of Theorem

Theorem 1. Gradient Vector Representation

Proof: Consider an arbitrary point X in the n-dimensional space. Let f denote the value of the objective function at the point X. Consider a neighbouring point $X + dX$ with

$$dX = \begin{pmatrix} dx_1 \\ dx_2 \\ . \\ . \\ . \\ dx_n \end{pmatrix}$$

where dx_1, dx_2, ..., dx_n represent the components of the vector dX. The magnitude of the vector dX, ds, is given by:

$$dX^T dX = (ds)^2 = \sum_{i=1}^{n} (dx_i)^2 \tag{A.1}$$

If $f + df$ denotes the value of the objective function at $X + dX$, the change in f, df, associated with dX can be expressed as:

$$df = \sum_{i=1}^{n} \frac{\delta f}{\delta x_i} dx_i = \nabla f^T dX \tag{A.2}$$

If $\mathbf{u}$ denotes the unit vector along the direction dX and ds the length of dX, we can write:

$$dX = \mathbf{u}ds \tag{A.3}$$

The rate of change of the function with respect to the step length ds is given by (A3) as :

$$\frac{df}{ds} = \sum_{i=1}^{n} \frac{\delta f}{\delta x_i} \frac{dx_i}{ds} = \nabla f^T \frac{dX}{ds} = \nabla f^T \mathbf{u} \tag{A.4}$$

The value of $\frac{df}{ds}$ will be different for different directions and we are interested in finding the particular step dX along which the value of $\frac{df}{ds}$ will be maximum. This will give the direction of the steepest ascent. In general, if the $\frac{df}{ds} = \nabla f^T \mathbf{u} > 0$ along a vector dX, it is called a direction of ascent, and if the $\frac{df}{ds} < 0$ it is called a direction of descent. By using the definition of the dot product,(A5) can be written as:

$$\frac{df}{ds} = \parallel \nabla f \parallel \parallel \mathbf{u} \parallel cos\theta \tag{A.5}$$

where $\parallel \nabla f \parallel$ and $\parallel \mathbf{u} \parallel$ denote the lengths of the vectors ∇f and $\mathbf{u}$, respectively, and θ indicates the angle between the vectors ∇f and $\mathbf{u}$. It can be seen that $\frac{df}{ds}$ will be maximum when $\theta = 0^0$ and minimum when $\theta = 180^0$. This indicates that the function value increases at a rate in the direction of the gradient in other words when $\mathbf{u}$ is along ∇f.

The rate of change of f with respect to the step length s along the direction $\mathbf{u}$ is given (A.5). Since $\frac{df}{ds}$ is maximum when $\theta = 0^0$ and $\mathbf{u}$ is a unit vector, then equation (A.6) gives $(\frac{df}{ds}) \mid_{max} = \parallel \nabla f \parallel$ which proves the theorem. Q.E.D

Theorem 2. Proof of Convergence of gradient descent

Most of the know iterative algorithms for solving unconstrained problems take the form:

$$p_{k+1} = p_k + a_k d_k \tag{A.6}$$

where a_k is scalar gain factor which is a positive step-size parameter and if $\nabla_k \neq 0$, d_k is descent direction;

It satisfies: $d_k^{'} \nabla_k < 0$ if $\nabla_k \neq 0$ and

$d_k = 0$ if $\nabla_k = 0$.

This kind of algorithm is referred to as a generalised gradient method or simply gradient method. Q.E.D.

Procedure for image registration for Images of Figure 3.1-3.3

Step 1: Find image rotation and scale:

Read both fixed and moving images

$fixed01 = imread('01_fixed.png')$;

$moving01 = imread('01_moving.png')$;

Convert to grayscale from RGB

$Image1 = rgb2gray(fixed01)$;

$Image2 = rgb2gray(moving01)$;

Step 2: Resize the image [0:255]

$A1 = imresize(Image1, 0.5)$;

$A2 = imresize(Image2, 0.5)$;

Make image A1 same size as image A2 using the following command in Matlab:

$All = imresize(A1, [NoR\ NoC]);$

$figureimshow(All)$

$title('Fixed01')$

$scale = 0.7;\ distorted - imresize(All, scale);$

$theta = 30;$

$distorted = imrotate(distorted, theta)$

$figure, imshow(distorted).$

Step 3: Select control points

$movingpoints = [x_{m1}y_{m1}\ x_{m2}y_{m2}\ ...\ x_{mn}y_{mn}];$

$fixedpoints = [x_{f1}y_{f1}\ x_{f2}y_{f2}\ ...\ x_{fn}y_{fn}];$

$cpselect(distorted, original, movingpoints, fixedpoints);$

Step 4: Estimate Transformation

$tform = fitgeotrans(movingpoints, fixedpoints,' affine');$

Step 5: Select the optimiser and metric

$Optimiser = registration.optimiser.One + OneEvolutionary;$

$Metric = registration.metric.MeanSquares;$

$Optimiser.MaximumIterations = 300;\ 500;\ 800;\ 1000;$

$Optimiser = registration.optimiser.One + OneEvolutionary;$

$Optimiser.InitialRadius = optimiser.InitialRadius/3.5;$

$movingRegistered = imregister(Image1, Image2,' Similarity', optimiser, metric);$

$movingRegisteredAdjustedInitialRadius = imregister(Image1, Image2,' Similarity', optimiser, met$

$figure, imshow(movingRegisteredAdjustedInitialRadius, Image2).$

$title('AdjustedInitialRadius')$

$tformSimilarity = imregtform(Image1, Image2,' affine', optimiser, metric);$

$Rfixed = imref2d(size(Image2));$

$movingRegisteredRigid = imwarp(Image1, tformSimilarity, OutputView, Rfixed);$

$figure, imshowpair(movingRegisteredRigid, Image1).$

$title('RegisteredAffineImage01').$